Manuscript Details

Manuscript number	SAFETY_2017_122
Title	Resiliency Assessment of Urban Rail Transit Networks: Shanghai Metro as an Example
Article type	Research Paper

Abstract

This paper presents a general framework to assess the resilience of large and complex metro networks by quantitatively analyzing its vulnerability and recovery rapidity within unifying metrics and models. The connectivity performance of network is indicated by the network efficiency. The resilience of a metro network can be associated to the network performance loss triangle over the relevant timeline from the occurrence of a random or intentional disruption to full recovery. The proposed resilience model is applied to the Shanghai metro network with its 303 stations and 350 links as an example. The quantitative vulnerability analysis shows that the Shanghai metro with its L-space type of topology has a strong robustness regarding connectivity under random disruption but severe vulnerability under intentional disruption. This result is typical for small-world and scale-free networks such as the Shanghai metro system, as can be shown by a basic topological analysis. Considering the case of one disrupted metro station, both the vulnerability and resilience of the network depend not only on the node degree of the disrupted station but also on its contribution to connectivity of the whole network. Analyzing the performance loss triangle and the associated cost from loss of operational income and repair measures, an appropriate recovery strategy in terms of the optimum recovery sequence of stations and the optimum duration can be identified in a structured manner, which is informative and helpful to decision makers.

Keywords	Network Resilience; Shanghai Metro; Node Connectivity; Topology; Robustness; Vulnerability.
Taxonomy	Metro Tunnels, Resilience, Transport Infrastructure
Manuscript region of origin	Asia Pacific
Corresponding Author	Hongwei Huang
Order of Authors	Dongming Zhang, Fei Du, Hongwei Huang, Fan Zhang, Bilal Ayyub, Michael Beer

Submission Files Included in this PDF

File Name [File Type]

Cover Letter for SS.doc [Cover Letter]

Response to Reviewer Comment-20170821.docx [Response to Reviewers (without Author Details)]

Highlights-20170821.doc [Highlights]

Abstract-20170821.doc [Abstract]

Title page-20170821.doc [Title Page (with Author Details)]

Revised Manuscript-without author details-20170821.doc [Manuscript (without Author Details)]

To view all the submission files, including those not included in the PDF, click on the manuscript title on your EVISE Homepage, then click 'Download zip file'.

Research Data Related to this Submission

There are no linked research data sets for this submission. The following reason is given:
Data will be made available on request

Professor Hongwei Huang

Room 722, Geotechnical Building, Tongji University

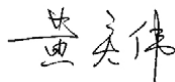Siping Road 1239

Shanghai 200092

P.R.China

Aug 21, 2017

Dear Editor,

Thank you very much for your letter dated June 14 2017 with regard to our manuscript entitled "**Resiliency Assessment of Urban Rail Transit Networks: Shanghai Metro as an Example (SAFETY_2017_122)**. Authors' special thanks also goes to the reviewers. All the comments and recommendations are quite insightful and valuable to improve the quality of our manuscript. According to the comments, we have checked the manuscript thoroughly and revised it carefully. Revised portion are marked in <mark>yellow</mark> in the revised manuscript. Detail responses to the comments can be found in the document named by "response to reviewers".

Should you need to contact me, please use the above address or call me at (86)-21-6598-9273. You may also contact me by fax at (86)-21-6598-5017 or via e-mail at huanghw@tongji.edu.cn

Sincerely,

Hongwei Huang

Ref: SAFETY_2017_122
Resiliency Assessment of Urban Rail Transit Networks: Shanghai Metro as an Example

Dear Editor,

We would like to thank the reviewers and editor for their time and their thoughtful comments. All the comments and recommendations are quite insightful and valuable to improve the quality of our manuscript. According to these comments, the manuscript has been thoroughly revised. The revised portion is marked in <mark>yellow</mark> in the revised manuscript. Detailed responses to the comments can be found below.

<u>Reviewer #1:</u>

1. Recommend restructuring sections or rewording the introduction to include a stronger framework with more succinct transitions between sections.

Reply:
Following the reviewer's very good suggestion, **the authors have revised the introduction to add transitions between sections and an explicit framework in the last paragraph of the introduction**.

Line 63 – 65: "*Quite a number of studies have been carried out by analyzing networks for the safety of metro systems in particular with the topographical mapping modelling (Crucitti et al., 2003; Derrible and Kennedy, 2010; Watts and Strogatz, 1998; Zhang et al., 2013; Zhang et al., 2011).*"

Line 78 – 81: "*The above network assessment models, however, are mainly qualitative with conceptualized measures that do not offer a rigorous comparison of safety levels among networks. In this respect, network analysis with quantitative measures of robustness and vulnerability is thus helpful for examining the safety level of a specific network.*"

Line 89 – 91: "*Additionally, disrupting a large-scale metro network by an accident affects not only the robustness but also the subsequent recovery. Recovery profiles over time greatly affect the economic and social wellbeing outcomes that are of great concern to metro owners.*"

Line 94 – 97: "*In the context of recovery, robustness and vulnerability analyses are still insufficient to offer a rational recovery strategy in terms of recovery sequencing and duration for stations and tunnels in a metro network.*"

Line 98 – 101: "*A comprehensive safety assessment model includes both the network robustness and the recovery profile as provided by Ayyub (2014). In this context, the concept of "resilience" would provide an appropriate solution to cover both the robustness and recovery in a single model for safety evaluation of a network system (Ayyub, 2015; Bruneau et al., 2003).*"

Line 124 – line 127: "*This paper provides a general framework for the resilience analysis of large-scale metro network systems that offers an immediate basis for identifying both the best recovery sequences to minimize the performance loss and the best repair duration to minimize the costs associated with disruption and recovery.*"

Line 135 – 141: "*The main body of the paper is provided in two subsequent primary sections. The first primary section provides the detailed description of the resilience model according to the above four items. The second primary section provides an application of the above resilience model to the Shanghai metro. Recovery strategies are discussed for (a) a single multi-line station, and (b) multiple stations in terms of repair sequences that minimize the resilience loss triangle. Then, a brief application example focusing on cost analysis during disruption and recovery is used to illustrate the concepts introduced. Finally, concluding remarks are presented.*"

2. While I do believe this study is fascinating and "worthy of investigation" I urge you to consider making a more substantive claim earlier in the paper demonstrating how findings in this study may have implications and applications outside of Shanghai.

Reply:

The reviewer's comment is quite appreciated. **Yes, the proposed resilience analysis model is suitable not only for the Shanghai case, but also for complex metro network systems of other big cities**, such as London, Beijing, New York, Paris, and etc. The Shanghai metro is only one example used in this paper for the purpose of demonstrating the application of the proposed model to such a complex metro network. **The authors have added the potential use of the proposed model explicitly in the last paragraph of introduction in line 141 – 144.**

"*Although the illustrative examples in this paper are based on the Shanghai metro, the proposed resiliency model is applicable for safety analysis of other complex metro networks, such as in London, New York, etc., with the emphasis on network robustness and recovery.*"

<u>-Reviewer 2</u>

Review comments
Manuscript number SAFETY_2017_122
Title: "Resiliency Assessment Model of Urban Rail Transit Networks: Shanghai Metro as an Example"

1. Title: Ok
2. Abstract: Clear and logical. Nicely point out the key findings of the results.
3. Keywords: Add "vulnerability"

Reply:
We have added the key word "Vulnerability" in the revised manuscript. Thanks for the good suggestion.

<u>4. Introduction</u>
(i) At p-5, the sentence "cost related to recovery stage should also be taken into account for a full assessment of the resiliency of the metro network" is mentioned. But this paper has not addressed the cost related recovery analysis.

Reply:

Yes, this is very important. We have revised the manuscript extensively to address this issue. Apart from proposing the general framework for resilience analysis, we now discuss the cost during disruption and recovery stage, however omit the cost-related analysis for the safe operation in lifetime of the metro system due to less relevance to the scope of the paper. For an optimized recovery strategy, when the best recovery sequence is determined by the proposed resilience model (i.e., maximizing the index Re), the key question for the decision maker is the best repair duration to be determined. Obviously, it should be related to the cost during the disruption and repair works. **Hence, the cost in this paper includes the disruption cost $C_{disruption}$ and the repair cost C_{repair}. Each component of the costs, i.e., $C_{disruption}$ and C_{repair}, is newly discussed extensively in the following:**

For disruption cost $C_{disruption}$, two major categories are analyzed in the conceptualized form, including: 1) disfunction of equipment and abandonment of facility in metro station; and 2) income and stocks loss due to close of metro operation. Taking the flood induced failure of metro station for an example, once the station is assumed to be disrupted by the severe flood, the equipment such as track barriers, escalator, signal board and etc., could be partially or totally disabled. Later on, the control rooms and power plant rooms might also be affected due to the floods. Furthermore, when the metro station is completely closed, the incomes including the tickets, the retails and other business around the metro stations might be lost. In addition, the stocks of the metro company will be further affected due to the disruptions. **All those cost factors are listed in Table 1 (newly added in the revised manuscript).** However, to incorporating all these factors in this study would be too complicated and straightforward for the decision-making. In this case, for ease of discussion, the cost analysis for $C_{disruption}$ in this manuscript is mainly based on the income loss of the tickets C_{ticket} ($C_{disruption}$ = C_{ticket} in this paper) which can be quantitatively evaluated. Those other cost factors in Table 1 could be related to the ticket income qualitatively with a coefficient ($C_{others} = \lambda \times C_{ticket}$) if interested in the next study.

For the repair cost C_{repair}, it includes the direct cost and indirect cost. The direct cost is related to the salary of workers, consumption of engineering materials, rental of the engineering machinery etc. Some typical direct costs are also shown in Table 1. For a certain repair project, shortening the repair duration t can be achieved by an increase of salary, the use of high quality materials, and more machinery. Hence, the direct cost is believed to be negatively correlated with the repair time duration t. The indirect cost is caused by social related factors (also shown in Table 1), which is believed to be positively correlated with the time duration t. **Hence, the repair cost is a typical time-cost trade-off problem which can be solved by the LP/IP hybrid method proposed by Liu et al. (1995).**

Table 1 Cost produced due to disruption of metro station

Cost Category		Content
Disruption cost	Disfunction of equipment	track
		track barrier
		escalator
		signal board
		ticket barrier
		air-conditioning system
		ventilation system
	Abandonment of facility	managing control room
		power plant room
		ventilation room
		signal system room
		escape shaft
	Income loss	metro ticket
		retail
		mall
		rental
		real estate
	Stocks	stocks
Repair Cost	Direct cost	salary of workers
		monitoring and inspection before repair
		site investigation
		construction materials
		rental of engineering machinery
		purchase of power, ventilation and signal system
	Indirect cost	time value
		social impact

The above detailed discussion on the cost and Table 1 are newly added in the revised manuscript.

Line 292 – line 298: "*The recovery of network connectivity is a primary goal for decision makers; however, disruption and repair costs associated with recovery profiles a key criterion in decision making. Once the recovery sequence is selected, the particulars of recovery plans, i.e., repair methods, equipment, etc., affect the repair duration and subsequently the recovery cost. Generally, advanced techniques for repair work require less time to complete recovery task, but at a greater cost. Hence, a recovery cost analysis in terms of repair time duration helps to determine the optimized cost of repair.*"

Line 303 – line 322: "*Following the basic model proposed by Henry and Ramirez-Marquez (2012), the total cost C_{total} during the disruption and repair stages is generally composed of two parts, namely the cost $C_{disruption}$ and the cost $C_{repairs}$, represented as:*"

$$C_{total} = C_{disruption} + C_{repair}$$

(11)

where the $C_{disruption}$ is referred to the cost or income loss due to the disruption of network connectivity and the

$C_{repairs}$ means the cost or investment for the repair works. Taking the flood-induced failure of metro station as an

example, the $C_{disruption}$ might include two major categories, i.e., damaged but repairable equipment and damaged

but non-repairable equipment, and income loss due to closing of metro operations. Once a station is set as

disrupted by flooding, the equipment such as track barriers, escalator, signal board and etc., could be partially or

totally disabled. Later on, the control rooms and power plant rooms might also be affected due to flooding.

Furthermore, when the metro station is completely closed, loss in income from ticket sales, the retails and other

business around the metro stations comes on top. In addition, the stocks or reputation of the metro company could be affected due to the disruptions. Details of the above disruption cost are shown in Table 1. However, incorporating all the factors shown in Table 1 for disruption cost $C_{disruption}$ requires data that are not available in some cases. For ease of discussion, the cost analysis for $C_{disruption}$ in this paper includes mainly the income loss in the ticket sales C_{ticket} ($C_{disruption} = C_{ticket}$ in this paper) which can be quantitatively evaluated. Some other cost factors in Table 1 could be related qualitatively to the ticket income using perhaps multiplication coefficients ($C_{others} = \lambda \times C_{ticket}$) as an example."

Line 406 – line 409: "*After determining the optimal repair sequence by the resilience analysis model as shown in Figure 4, the optimal repair duration for each station could be obtained from the above cost analysis. Therefore, the best recovery strategy due to the disruption can be achieved both with the best recovery sequence and duration.*"

Overall, the philosophy behind the recovery strategy for disrupted metro system is first to select a best recovery sequence and second to select a best repair duration considering both the disruption and repair cost. **In order to show the application of the above cost analysis, an example of cost analysis for recovering a completely disrupted metro station by rebuilding a new station is discussed in the revised manuscript**:

Line 531 – line 539: "*Furthermore, repair duration should be optimized on the basis of minimizing the disruption and repair costs. The philosophy behind the recovery strategy for a disrupted metro system is first to select the best recovery sequence either for an exchange station or for multiple stations and second to select the best repair duration considering both the disruption and repair cost. In this regard, the following section shows an example of three typical cases of the resilience analysis of the Shanghai metro network: Case 1 is to obtain the best recovery sequence for a disrupted exchange station; Case 2 is to obtain the best recovery sequence for multiple disrupted stations; and Case 3 is to obtain the best repair duration for rebuilding a disrupted metro station.*"

Line 621 – line 665:

"**Case 3: Recovery cost to rebuild a disrupted metro station**

In this hypothetical example, a metro station is disrupted completely at time t_0 and requires rebuilding of the damaged station. For ease of discussion, t_0 is assumed to be zero. In addition, time-value of money is not considered in this example for simplicity. During the repair procedure, the metro station is closed to the public. As mentioned previously, the disruption cost in the recovery stage is assumed to only include the income loss related to metro tickets. From the statistics of the Shanghai metro, the daily passenger flow volume is more than 10 million. Hence, the disruption of one station among the 303 stations of the whole network is assumed to lead in a loss of about 40 thousand passengers flow volume every day. The ticket price of Shanghai metro is about 4 RMB on average. For this case, from Eq. 13b, the disruption cost during the recovery procedure can be calculated as below:

$$C_{disruption} = \frac{1}{2} \times 4 \times 40000 \left(t_1 - t_0 \right)$$

(15)

where t_1 is the recovered time moment that is unknown and needs to be optimized and t_0 is equal to zero that is assumed in this example.*

The rebuilding of a metro station requires several stages in sequence, including the site investigation, construction of a pile foundation of underground structures, construction of a soil retaining system, soil excavation with construction of supports and dewatering, and construction of underground structures of the metro station. From personal communication with the managers in charge of design, construction and operation, Table 8 shows a typical example of repair options associated with the direct cost and duration for rebuilding one typical metro station in Shanghai. It is quite obvious from direct cost perspectives that the shorter the repair duration, the higher the cost. Solving such a typical time-cost tradeoff requires the use of linear and integer programming (LP/IP) models, such as Liu et al. (1995). Table 9 shows the calculated results of repair duration and associated direct cost of

construction. The indirect cost is assumed, in this example, to be equal to 100 thousands RMB per day. Hence, the total indirect cost can also be calculated based on the calculated duration, as shown in Table 9. Figure 14a shows the calculated direct cost, indirect cost and the repair cost against the repair duration, respectively (solid circles for C_{repair}, hollow triangles for direct cost and hollow rectangles for indirect cost). It is observed from Figure 14a that the optimized repair duration based on repair cost is around 455 days. Corresponding to this calculated repair duration, the disruption cost in terms of the ticket income loss can be derived from Eq. 15, as displayed in Table 9. Hence, the total cost C_{total} both including $C_{disruption}$ and C_{repair} can be obtained as shown in Figure 14b (solid circles for C_{total}, hollow circles for C_{repair} and hollow rectangles for $C_{disruption}$). The optimized repair duration after incorporating the income loss is about 450 days, which is less than the optimized duration considering only repair cost. This finding is reasonable, as the income loss will continue to increase when the repair work is not finished. In this example, the disruption cost only includes the ticket income loss, resulting in a five-day decrease of the optimized duration. Although the number of days in this case is small, the best repair duration might be reduced further as other cost elements of disruption are considered. If the other disruption cost as shown in Table 1 is considered to be proportional to the ticket income loss, i.e., $\lambda = (C_{disruption}\text{-}C_{ticket})/C_{ticket}$, Figure 14c has illustrated the effect of parameter λ on the optimized repair duration days. It is clear that as the λ becomes larger, i.e., that is to say, the other disruption cost increases, the optimized repair duration days would be greatly reduced. It is consistent with the engineering practice that if the disruption cost is invaluable or social effect of the metro accident is unacceptable, the best repair strategy should be as fast as possible."

Table 8 Repair options for rebuilding a metro station in Shanghai

Procedure	Options	Cost (million RMB)	Duration (day)
Site investigation	crew1+equipment1	6	50
	crew2+equipment2	8	40
Pile foundation	crew1+equipment1	6	30
Retaining wall	crew1+equipment1	29	80
	crew2+equipment2	33	70
Excavation /support /dewatering	crew1+equipment1	15	180
	crew2+equipment2	20	165
Underground structure	crew1+equipment1	30	120
	crew2+equipment2	35	110

Table 9 Integrated repair duration and cost for rebuilding a metro station in Shanghai

Duration (day)	C_{repair} Direct Cost	Indirect cost	sum	$C_{disruption}$	C_{total}
415	102.0	41.5	143.5	33.2	176.7
420	98.5	42.0	140.5	33.6	174.1
425	95.1	42.5	137.6	34.0	171.6
430	92.5	43.0	135.5	34.4	169.9
435	90.9	43.5	134.4	34.8	169.2
440	89.5	44.0	133.5	35.2	168.7
445	88.0	44.5	132.5	35.6	168.1
450	87.0	45.0	132.0	36.0	168.0
455	86.4	45.5	131.9	36.4	168.3
460	86.0	46.0	132.0	36.8	168.8

Note: cost unit is million RMB.
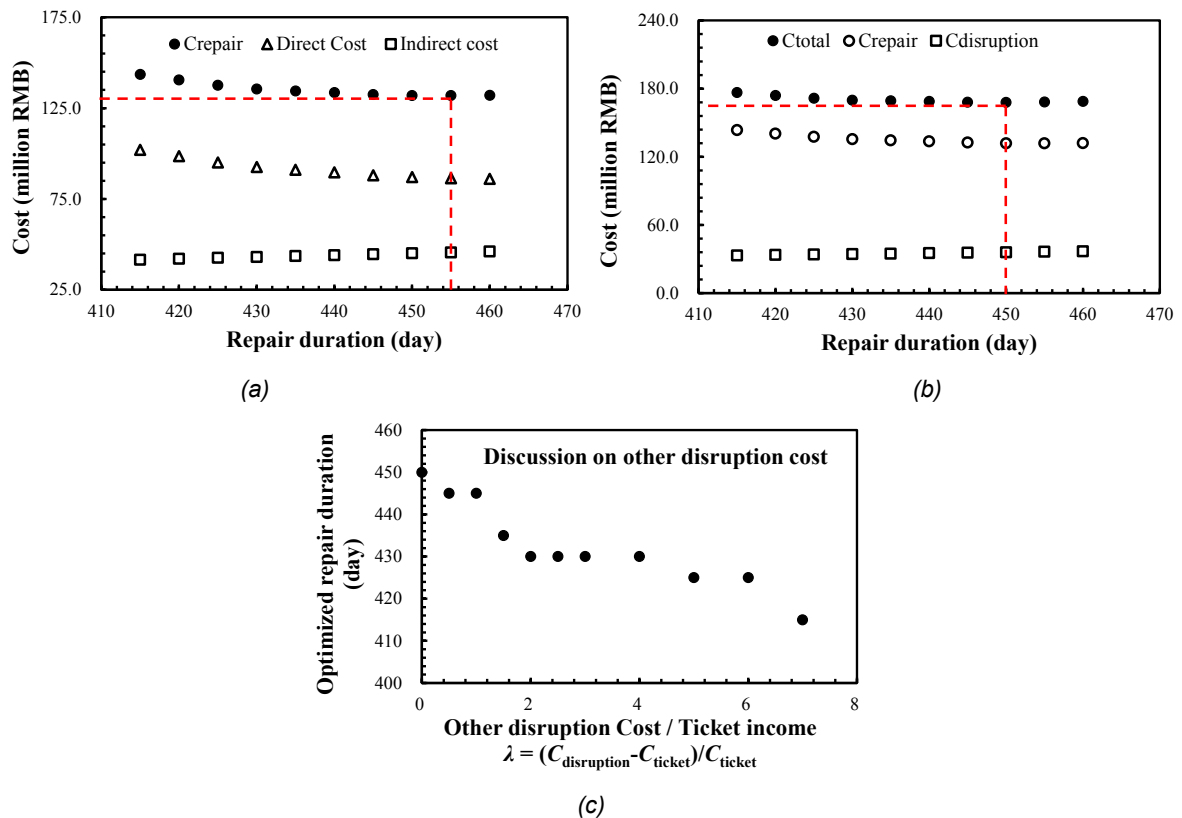
(a)

(b)

(c)

Figure 14 Time-cost trade-off analysis for rebuilding a metro station: a) time-cost for repair cost; b) time-cost for total cost including disruption cost and repair cost; and c) effect of other disruption cost on the optimized repair duration days "

(ii) The paper has discussed on the cost related to disruption and recovery stage; but has not contributed in the cost-related analysis.

Reply:
We thank the reviewer's understanding of the cost analysis discussed in the manuscript that is mainly for the disruption and recovery stage.   The detailed responses could be referred to the response to _the comment (i) in 4. introduction._

(iii) At p-5, in the second paragraph, it is not clear why repair measures are mentioned along with recovery measure? It is not discussed at all.

Reply:
Sorry for the wording mistake in the original version of the manuscript. **We have deleted the sentence to avoid the confusion of miswording**.

**5. General framework**
(i) Citation error in "Von Ferber et al. (2009)". It is not matched with the one in reference section.

Reply:
Thanks for the careful check of the citation. We have double checked with the original reference. The correct citation should be von Ferber et al. (2009). Hence, the name for author von Ferber is corrected in the revised manuscript.

(ii) In this and subsequent sections, there should be Figure 1 or 2 or 3, etc.; not Fig. 1, 2, or 3.

Reply:
We have revised all the figure captions in the text following the reviewer's suggestion.

(iii) In citation, it is shown that authors used "Zhang, et al., 2011", which should be "Zhang et al., 2011". Extra comma comes up after the first author's surname, which should not be there as per APA style.

Reply:
Thanks for the reviewer's kindly reminder. We have read through the formatting requirement for the citation for the journal "Safety Science". We revised all the citations with et al. in the text.

(iv) At p-8, explain briefly power curve.
(v) Provide reference for the value range in .

Reply:
For a scaled-free network, the distribution *P(k)* of node degree *k*, i.e., the relative frequency of node degree *k*, would have a power law with the node degree *k*. The general power law could be represented by Eq. 5 in the manuscript. **The parameter α and γ are the regression coefficients to obtain a best-fitted pow curve between node degree *k* and its distribution *P(k)* for a specific network.** Literatures have indicated the exponent parameter γ usually ranges from 2.1 to 4 (Barabasi and Albert,1999). Hence, we have revised the description of Eq. 5 in the revised text:

Line 193 – line 197: "*The scale-free network is a network that has a distribution of node degrees P(k), i.e., the relative frequency of node degree k, following a power distribution:*

$$P(k)=\alpha k^{-\gamma}$$

(5)

where the parameters α and γ are the regressed coefficients for the power curve of a specific network. The value of γ usually ranges from 2.1 to 4.0 (Barabasi and Albert, 1999)."

The corresponding reference is added after the typical range.

Reference:
Barabasi, A.L., Albert, R., 1999. Emergence of scaling in random networks. Science 286, 509-512.

(vi) At p-10, citation error is noticed in "Bruneau et al (2003)", where full stop should come up after "al".

Reply:
We have revised the citation. Thanks for the careful check.

(vii) At p-10, in the line 216, the sentence "Hence, for an original metro network without failure....." is not complete.

Reply:
Sorry to misleading the sentence by inappropriate separation. We have re-worded the sentences for the readability in the revised text:

Line 244 – line 246: "*Hence, the magnitudes of robustness and vulnerability of a network depend on the node that is disrupted. By examining all the nodes, one at a time, robustness and vulnerability could indicate the order of importance of these metro stations for the network.*"

(viii) At p-12, in the second line from the top, the sentence "... some of the metro stations are interchanges...." has grammatical mistake.

Reply:
We have reworded this sentence as the reviewer suggested.

(ix) At p-12, Figure 3 should be explained clearly with the proper sequence of a to d, which is not maintained.

Reply:
Thanks for the good suggestion. The authors have added the description of the sequence for recovery in Figure 3. The figures are re-ordered accordingly.

Line 282 – line 284: "*A typical sequence is shown in Figure 3 with the first stage to recover Line 2 (Figure 3c), the second to recover Line 1 (Figure 3d) and the last stage to recover Line 3 to its original state (Figure 3a).*"

(x) The sub-section 2.4 should have the sub heading "Cost during disruption & recovery stage for a full Decision Making", not for recovery stage only.

Reply:
We have replaced the sub-heading following the reviewer's suggestion to "**2.4 Cost during Disruption and Repair Stage for a Full Decision Making**"

(xi) Typo is found at p-13 in the serial paper line number 282, "ticket prize" is written, which should be "ticket price".

Reply:
We are sorry for the typo error.   The revised manuscript has been carefully checked to avoid such kind of error again.

(xii) At p-14 in the paper line number 294, recovery function was taken as linear, which in real cases is hardly observed.

Reply:
The authors have to admit that such kind of recovery of passenger flow volume is hardly observed neither in linear form nor in other non-linear form.   It is difficult to evaluate precisely the recovery procedure for passenger flow even after the re-open of the recovered station.   However, **for the recovery of multiple stations, it should make sense that the recovery of the passenger flow is a step function which can be approximately modelled by the linear function for simplicity in calculation**.   Overall, for the purpose of the calculation of the disruption cost, the recovery curve of passenger flow volume is assumed to be linear as none of other nonlinear curves is evident.

(xiii) At p-16 at paper line number 345, full form of "PV" is not mentioned.

Reply:
$C_{total, PV}$ means the present value (PV) equal to the total cost C_{total} at time of full recovery ($t = t_1$).   It should be less than the value of money exactly at present (C_{total}).   The text in page 16 has been revised and the notation $C_{total, PV}$ is explained in detail in notations section.

Line 400 – line 401: "*…(present value equal to the total cost at time t_1, i.e., $C_{total, PV}$)…*"

Line 734: " $C_{total, PV}$ *Present value equal to the total cost at time of recovery* "

6. Application of the Resilience Model....
(i) At p-19, paper line number 412, calculation of is not shown. Consequently, it makes it unclear for the readers.

Reply:
We are sorry to make the reviewer unclear about the calculation of network connectivity.   Basically, the network connectivity E_f is calculated based Eq. 6.   The node number N is 303 for an initial network without failure.   The path length d_{ij} for all pair nodes in the network is calculated by using the Floyd algorithm (Floyd, 1962) from the correlation matrix A.   Since the calculation requires repeated searches for shortest path length, a Matlab-based code is used.   The authors could share the Matlab function codes if the reviewer is interested.

In addition, the text in the manuscript has been newly revised in:

Line 174 – line 177: "*There are quite a number of classical algorithms to calculate the path length d_{ij} efficiently from the correlation matrix A, e.g., Dijkstra's algorithm, Bellman-Ford algorithm, Floyd algorithm (Zhan and Noon, 1998).*"

Line 462 – line 466: "*The initial network connectivity E_f without any failure is calculated by using Eq. 6, where the node number N is equal to 303 and the path length d_{ij} for all pair nodes in network is calculated by using the Floyd algorithm (Floyd, 1962).   The calculated E_f is equal to 0.0994.   After the disrupted node is removed, the similar procedure of calculation could be repeated for a disrupted network as described above.*"

Reference:
Floyd, R.W., 1962. Algorithm 97 (Shortest Path). Communications of the Acm 5, 345-345.
Zhan, F.B., Noon, C.E., 1998. Shortest path algorithms: an evaluation using real road networks. Transportation science 32: 65-73.

(ii) At the same page in paper line number 420, inflection point is mentioned as 0.3. It is not clearly mentioned in the figure. In text, its significance is not discussed, as well how it is obtained?

Reply:
We appreciate the reviewer's good suggestion on the elaboration of inflection point in Figure 10.   By drawing two extension lines for the two distinct stage of network efficiency shown in Figure 10 (the variation of network efficiency approximately appears to be linear for each stage), the intersection point could be regarded as the inflection point.   The inflection point for intentional attack is about 0.10, while for random attack is about 0.24.   Obviously, the inflection point for random attack is greatly moving to the right side of the inflection point for intentional attack.   It clearly shows the robustness of the metro network under the condition of random attack.   **Correspondingly, the text has been revised in the manuscript in**:

Line 478 – line 480: "*By drawing two extension lines (black dash line in Figure 10) along these two distinct stages, the intersection of these two lines could be regarded as the inflection point.   *"

Line 485 – line 488: "*The inflection point for random attack is greatly moving to the right side of the inflection point for intentional attack.   It clearly shows that the robustness of the metro network under the condition of random attack is much better than the robustness under the condition of intentional attack.*"

In addition, Figure 10 is also re-drawn to explicitly show the inflection point.

(iii) At p-20 in the paper line number 442, calculation of original connectivity is not shown.

Reply:
Thanks for the reviewer's comment.   Details of the calculation for original connectivity could be referred to the response to *comment (i) in 6. Application of the Resilience Model.*

(iv) At p-22 in the paper line number 485, one small calculation of should be shown for better understanding by the readers.

Reply:
Thanks for the reviewer's rigorous point of view on the calculation of resilience index Re. Basically, the calculation is carried out using Eq. 10.   **A typical calculation example is newly added in the revised manuscript to explicitly show the calculation procedure for ease of understanding.**

Line 557 – line 563: "*Considering the recovery sequence 2-6-9-4 as an example, the calculated initial network connectivity is equal to 0.0994, and the network connectivity after the disruption of the station is 0.0932.   After recovery according to the sequence 2-6-9-4, the network connectivity is gradually increased from 0.0932 to 0.0953 (Line 2 is recovered), to 0.0973 (Lines 2 and 6 are recovered), to 0.0985 (Lines 2, 6 and 9 are recovered), and to 0.0994 (fully recovered for Lines 2, 6, 9 and 4).   Hence, by using Eq. 10, the resilience index R_e is   calculated to be 0.974, i.e., 0.974   = 0.5 × (0.0932 + 2 × 0.0953 + 2 × 0.0973 + 2 × 0.0985 + 2 × 0.0994) × 4 / (4×0.0994).*"

(v) At p-22 in the paper line number 492, the significance of "Stage zero" has not been discussed.

Reply:
Thanks for the reviewer's good suggestion on the description of stage zero in the text.   **We have revised the text in line 570 – line 572**:

"*Stage zero stands for a metro network in its normal state without any disruption.   The initial network efficiency as calculated in the robustness analysis is about 0.0994.*"

(vi) For both the example cases, cost has not been taken whereas the authors admit that cost factors should be considered for a full assessment of the resiliency of the metro networks (see p-5 at paper line numbers 99-101) which is the prime focus of this current study.

Reply:
Thanks for the reviewer's suggestion. The potential contribution of this manuscript, in the authors' opinion, should be twofold, i.e., the first and most important one is the resilience model and its associated metric for determining the recovery sequence, and the second one is the additional cost analysis to assist the recovery strategy after selecting a best recovery sequence. With this idea in mind, the authors have added one more example for cost analysis in the revised manuscript. Details of the example could be referred to the response to *the comment (i) in 4. Introduction*.

7. Reference
(i) The only reference mentioned at line number 643 needs to be changed to the same style used for other referencing.
(ii) The reference mentioned at the page line number 673, check which one is correct whether "Von..." or "von...".

Reply:
The formatting of the reference has been double checked and revised following the suggestion.

8. Overall:
The paper though presents a nice contribution towards bridging the gap in resiliency assessment model for urban rail transit networks; however, it has some serious limitations that should be discussed appropriately. For example, why the cost factors are not considered needs to be explained clearly. In addition, the logic behind the assumptions made in this paper has to be provided. Further, many typos, referencing, grammar, etc. need to be corrected.

Reply:

First of all, the authors are greatly appreciated for the reviewer's insightful comments, which definitely has improved the quality and rigorousness of the manuscript. For each comment, we have made a thorough revision and detailed responses. We hope the manuscript now is clear and meet the requirement of the journal.

Highlights:

1. A general framework to quantitatively assess resilience of complex metro network by analyzing its vulnerability and recovery rapidity is proposed in this paper.

2. The best recovery strategy in terms of optimum recovery sequence of stations and optimum duration can be identified in a structured manner.

3. Shanghai metro system is a typical small-world and scale-free network with strong robustness of connectivity under random disruption but severe vulnerability under intentional disruption.

1 **Resiliency Assessment of Urban Rail Transit Networks: Shanghai Metro as an**

2 **Example**

3

4 **Abstract:** This paper presents a general framework to assess the resilience of large and complex

5 metro networks by quantitatively analyzing its vulnerability and recovery rapidity within

6 unifying metrics and models. The connectivity performance of network is indicated by the

7 network efficiency. The resilience of a metro network can be associated to the network

8 performance loss triangle over the relevant timeline from the occurrence of a random or

9 intentional disruption to full recovery. The proposed resilience model is applied to the Shanghai

10 metro network with its 303 stations and 350 links as an example. The quantitative vulnerability

11 analysis shows that the Shanghai metro with its L-space type of topology has a strong robustness

12 regarding connectivity under random disruption but severe vulnerability under intentional

13 disruption. This result is typical for small-world and scale-free networks such as the Shanghai

14 metro system, as can be shown by a basic topological analysis. Considering the case of one

15 disrupted metro station, both the vulnerability and resilience of the network depend not only on

16 the node degree of the disrupted station but also on its contribution to connectivity of the whole

17 network. Analyzing the performance loss triangle and the associated cost from loss of

18 operational income and repair measures, an appropriate recovery strategy in terms of the

19 optimum recovery sequence of stations and the optimum duration can be identified in a

20 structured manner, which is informative and helpful to decision makers.

21

Resiliency Assessment of Urban Rail Transit Networks: Shanghai Metro as an Example

1

2 **Example**

3

4 **Dong-ming Zhang**

5 Assistant Professor, Department of Geotechnical Engineering, Tongji University, Shanghai,

6 China. Email: 09zhang@tongji.edu.cn

7 **Fei Du**

8 Master of Engineering, Department of Geotechnical Engineering, Tongji University, Shanghai,

9 China. Email: dufei1530755@tongji.edu.cn

10 **Hongwei Huang**

11 Professor, Department of Geotechnical Engineering, Tongji University, Shanghai, China, Email:

12 huanghw@tongji.edu.cn (*Corresponding author*)

13 **Fan Zhang**

14 Master of Engineering, Bureau Veritas Investment (Shanghai) Co., Ltd, Shanghai, China, Email:

15 zhangfanld@126.com

16 **Bilal M. Ayyub**

17 Professor, Center for Technology and Systems Management and Department of Civil and

18 Environmental Engineering, University of Maryland, MD, USA. Email: ba@umd.edu.

19 **Michael Beer**

20 Professor, Institute for Risk and Reliability, Leibniz Universität Hannover, Germany; Institute

21 for Risk and Uncertainty, University of Liverpool, UK; Shanghai Institute of Disaster Prevention

22 and Relief, Tongji University, Shanghai, China

23 beer@irz.uni-hannover.de

1   **Resiliency Assessment of Urban Rail Transit Networks: Shanghai Metro as an**

2   **Example**

3

4   **Abstract:** This paper presents a general framework to assess the resilience of large and complex

5   metro networks by quantitatively analyzing its vulnerability and recovery rapidity within

6   unifying metrics and models. The connectivity performance of network is indicated by the

7   network efficiency. The resilience of a metro network can be associated to the network

8   performance loss triangle over the relevant timeline from the occurrence of a random or

9   intentional disruption to full recovery. The proposed resilience model is applied to the Shanghai

10   metro network with its 303 stations and 350 links as an example. The quantitative vulnerability

11   analysis shows that the Shanghai metro with its L-space type of topology has a strong robustness

12   regarding connectivity under random disruption but severe vulnerability under intentional

13   disruption. This result is typical for small-world and scale-free networks such as the Shanghai

14   metro system, as can be shown by a basic topological analysis. Considering the case of one

15   disrupted metro station, both the vulnerability and resilience of the network depend not only on

16   the node degree of the disrupted station but also on its contribution to connectivity of the whole

17   network. Analyzing the performance loss triangle and the associated cost from loss of

18   operational income and repair measures, an appropriate recovery strategy in terms of the

19   optimum recovery sequence of stations and the optimum duration can be identified in a

20   structured manner, which is informative and helpful to decision makers.

21

1. Introduction

Urban rail transit systems (named subsequently as metro systems) offer an effective solution for addressing transportation problems in cities by significantly increasing the capacities of public transportation. This benefit has driven an expeditious development in the construction and operation of metro systems in many metropolitan cities. As the number of metro lines increases, metro systems often grow to a large and complex network scale. For example, Shanghai has a metro system with 303 stations and 350 tunnels over 617km. Although a large-scale metro network makes public transportation attractive and convenient, any accident impacting this mega system would greatly affect not only the serviceability of this critical infrastructure but also the safety of passengers. For example, in September of 2011, a signal failure occurred in a station of metro line 10 in Shanghai, China. Two metro trains crashed in a tunnel due to the loss of signal causing 271 injured passengers and 30-hour halt of the whole metro line (Mu, 2011). In view of these circumstances, the safety of metro networks is a key concern that requires an enhanced understanding of these networks through extensive research.

Quite a number of studies have been carried out by analyzing networks for the safety of metro systems in particular with the topographical mapping modelling (Crucitti et al., 2003; Derrible and Kennedy, 2010; Watts and Strogatz, 1998; Zhang et al., 2013; Zhang et al., 2011). Essentially, a metro network can be mapped into a topological graph with the simplification of metro tunnels and metro stations, respectively, as links and nodes used in topology (Zhang et al., 2013). Topological analysis, i.e., consisting of nodes and links, the path length and cluster coefficient of a network provides an effective and logical basis to characterize the safety of a transportation network (Derrible and Kennedy, 2010). Watts and Strogatz (1998) proposed a model termed *small-world network* for complex network analysis. The small-world network

48 system is typically highly clustered and yet have small characteristic path lengths, which

49 conceptually shows a robust connectivity of the nodes for a network subjected to any disruption.

50 Barabasi and Albert (1999) investigated large-scale networks and found that the node

51 connectivity in those networks, i.e., network connectivity, often follows a scale-free power-law

52 distribution. This result suggests that the connectivity of the network is robust under a random

53 failure yet is vulnerable under an intentional attack.

54 The above network assessment models, however, are mainly qualitative with conceptualized

55 measures that do not offer a rigorous comparison of safety levels among networks. In this

56 respect, network analysis with quantitative measures of robustness and vulnerability is thus

57 helpful for examining the safety level of a specific network. Albert et al. (2000) quantitatively

58 analyzed the robustness of metro networks in the event of an accident. The robustness of a metro

59 network here is expressed in terms of the residual network connectivity after the disruption of

60 nodes in the network. Crucitti et al. (2004) also studied the robustness of two types of large-

61 scale networks, i.e., a random network and scale-free network, for the performance of network

62 connectivity. These two studies revealed that scale-free networks have a high robustness index

63 under random attacks but a low robustness index under intentional attacks. Recently, a similar

64 analysis of the robustness of metro networks was also reported by Zhang et al. (2011) and Yang

65 et al. (2015). Additionally, disrupting a large-scale metro network by an accident affects not

66 only the robustness but also the subsequent recovery. Recovery profiles over time greatly affect

67 the economic and social wellbeing outcomes that are of great concern to metro owners. The

68 rapid recovery of a network's connectivity from a disrupted state to the normal state is a key

69 concern among engineers (Francis and Bekera, 2014). However, a robustness assessment

70 focuses only on the network safety in the event of an accident without considering recovery. In

71 the context of recovery, robustness and vulnerability analyses are still insufficient to offer a

72 rational recovery strategy in terms of recovery sequencing and duration for stations and tunnels

73 in a metro network.

74   A comprehensive safety assessment model includes both the network robustness and the

75 recovery profile as provided by Ayyub (2014). In this context, the concept of "*resilience*" would

76 provide an appropriate solution to cover both the robustness and recovery in a single model for

77 safety evaluation of a network system (Ayyub, 2015; Bruneau et al., 2003).   Resilience,

78 according to U. S. Presidential Policy Directive (PPD-21, 2013), means "*the ability to prepare*

79 *for and adapt to changing conditions and withstand and recover rapidly from disruptions.*"

80 Fundamentally, the resilience of a system is often quantified by relating it to a resilience loss

81 triangle represented by the difference between a normal performance evolution curve and a

82 disrupted performance curve along with the time duration of disruption and recovery stage

83 (Frangopol and Soliman, 2015). A resilient system can be quantitatively defined by the system

84 with a minimized performance loss triangle, also termed resilience loss triangle. The optimized

85 recovery sequences and duration necessary to minimize the resilience triangle thus offer a basis

86 for defining recovery strategies after disruptions (Zhang and Wang, 2016).

87   The concept of resilience as used herein was initially and formally introduced by Holling

88 (1973) for ecologic systems. Later on, a broader interest in resilience was triggered by the 2001

89 World Trade Center attack in the United States. Typical uses of resilience analysis has covered

90 mostly water resource systems (Hashimoto et al., 1982), power networks (Henry and Ramirez-

91 Marquez, 2012) and the seismic hazards for bridges (Dong and Frangopol, 2015). Resilience

92 analysis for urban rail transit systems, however, has been quite limited. On the other hand,

93 resilience analysis is of great necessity and importance in order to identify optimized recovery

94　sequences after network disruptions. One might realize that a metro network, to some degree, is

95　similar to the power network but with a different topological space of nodes and links and a

96　different recovery philosophy in terms of sequence and timing. These similarities can be

97　exploited in the development of respective approaches. In addition, the current practice of

98　recovery is purely based on empirical judgement without a rational model to obtain an optimum

99　repair duration and costs during the recovery stage (Huang and Zhang, 2016).

100　　This paper provides a general framework for the resilience analysis of large-scale metro

101　network systems that offers an immediate basis for identifying both the best recovery sequences

102　to minimize the performance loss and the best repair duration to minimize the costs associated

103　with disruption and recovery. The performance of a metro network in this paper refers to the

104　connectivity of stations in an integrated metro network (hereafter termed network connectivity).

105　The development of this framework requires the introduction of several concepts and models in

106　the context of metro networks as follows:

107　　1. Basic mapping of a metro network into a topological graph;

108　　2. Defining and measuring vulnerability and robustness of the topological metro network;

109　　3. Developing resiliency metrics based on the topological metro network;

110　　4. Accounting for costs during the disruption and recovery stage.

111　The main body of the paper is provided in two subsequent primary sections. The first primary

112　section provides the detailed description of the resilience model according to the above four

113　items. The second primary section provides an application of the above resilience model to the

114　Shanghai metro. Recovery strategies are discussed for (a) a single multi-line station, and (b)

115　multiple stations in terms of repair sequences that minimize the resilience loss triangle. Then, a

116　brief application example focusing on cost analysis during disruption and recovery is used to

117   illustrate the concepts introduced. Finally, concluding remarks are presented. Although the

118   illustrative examples in this paper are based on the Shanghai metro, the proposed resiliency

119   model is applicable for safety analysis of other complex metro networks, such as in London,

120   New York, etc., with the emphasis on network robustness and recovery.

121   **2. Proposed General Framework: Resilience Models for Large Metro Networks**

122   ***2.1 Topological Mapping of Metro Networks***

123   Several types of topological graphs are suitable to model transportation networks and systems

124   based on the use of nodes and links among nodes. von Ferber et al. (2009) summarized four

125   types of topological graphs, specifically, L-space type, B-space type, P-space type and C-space

126   type, for representing a typical bus transportation network. Among all these models, preference

127   is given to the L-space type graph for metro networks since it provides clear definitions in

128   relation to transportation networks. Nodes stand for bus stops and links among nodes stand for

129   connections between two successive bus stops of a bus line. A similar treatment can be adopted

130   for a metro system as graphically illustrated in Figure 1. Figure 1a shows an example of a metro

131   network. Each node represents a metro station, while a link between nodes stands for a metro

132   tunnel. Different metro lines are marked with different colors. Figure 1b is a typical L-space

133   topological graph for the metro network shown in Figure 1a.

134   A topological graph for a metro network can be expressed by a vector G:

135 $$G = [S, E] \tag{1}$$

136   where S is the node set for all the stations in a metro network, denoted as $S=[s_i|i=1, 2, 3, …, N]$

137   (N is the total number of stations), and E is the set of links for all the tunnels in the metro

138   network, denoted as $E=[e_{ij}|i, j \in S]$. The state of connection between any two nodes in a network

139   can be represented by a correlation matrix A, denoted as $A=[a_{ij}]_{N \times N}$. If nodes s_i and s_j are not

140 connected directly, then a_{ij} is equal to infinity. If there is a link between them, then a_{ij} is equal to

141 one. If i is equal to j, then a_{ij} represents the connection of a node with itself, which is set to zero.

142 In the topological analysis of the metro system in this paper, factors such as upper and lower

143 lines, link distance between stations, departure frequency of metro trains, passenger capacity and

144 the political reasons are not weighted in the network. The model used essentially results in an

145 undirected and unweighted network system, which is frequently used to represent the

146 transportation network system.

147   For the topological network of a metro system, the node degree k_i stands for the number of

148 nodes that have a direct connection with the node s_i. The average degree k^* is defined as the

149 average of the node degrees k_i for all nodes in the network. The minimum number of nodes that

150 need to be passed through from node s_i to node s_j is named path length d_{ij}. There are quite a

151 number of classical algorithms to calculate the path length d_{ij} efficiently from the correlation

152 matrix A, e.g., Dijkstra's algorithm, Bellman-Ford algorithm, Floyd algorithm (Zhan and Noon,

153 1998). The characteristic path length L is defined as the average over all path lengths d_{ij} for all

154 pairs of nodes (s_i, s_j) in a network:

155
$$L = \frac{1}{N(N-1)} \sum_{i \neq j} d_{ij} \tag{2}$$

156   Correspondingly, the diameter of a network D is defined as the maximum path length d_{ij}

157 among all pairs of nodes (s_i, s_j). The clustering coefficient C_i is defined as the ratio of the

158 number of links e_i between node s_i and its adjacent total of k_i nodes with respect to the maximum

159 possible number of links $k_i(k_i-1)/2$:

160
$$C_i = \frac{e_i}{k_i (k_i - 1) / 2} \tag{3}$$

161 The network-clustering coefficient C is the mean of all clustering coefficients C_i for all the

162 nodes.

163   By using the above basic notations, two typical properties of a topological network can be

164 characterized; the small-world property and the scale-free property. A small-world network is a

165 network that has a high network clustering coefficient C but is characterized by a small path

166 length L. A network is called a small-world network if

167
$$L > \frac{\ln(N)}{\ln(k^*)} \tag{4a}$$

168
$$C < \frac{k^*}{N} \tag{4b}$$

169 From a physical point of view, a small-world network possesses a reasonable local connectivity

170 (Barabasi and Albert, 1999). The scale-free network is a network that has a distribution of node

171 degrees $P(k)$, i.e., the relative frequency of node degree k, following a power distribution:

172
$$P(k) = \alpha k^{-\gamma} \tag{5}$$

173 where the parameters α and γ are the regressed coefficients for the power curve of a specific

174 network. The value of γ usually ranges from 2.1 to 4.0 (Barabasi and Albert, 1999). Generally

175 speaking, the power distribution of node degree means that the network has a few nodes with

176 large node degrees, and most of the nodes possess small node degrees.

2.2 Robustness and Vulnerability of Metro Networks

178   For a large-scale metro network, the connectivity from one station to another should be a key

179 criterion for metro operation. Once a metro network experiences a disrupting event, whether due

180 to degradation, human errors or intentional attack, the node connectivity would inevitably

181 decrease. The robustness of a metro network is its ability to resist and maintain residual node

182 connectivity after such an event. Hence, before evaluating network robustness, the node

8

183 connectivity needs to be characterized first. The network efficiency E_f is usually defined as an

184 indicator to quantify the node connectivity of a topological network (Latora and Marchiori,

185 2001):

$$E_f = \frac{1}{N(N-1)} \sum_{i \neq j} \frac{1}{d_{ij}}$$

186 (6)

187 where d_{ij} is the path length between nodes s_i and s_j. The inverse of path length d_{ij} essentially

188 means the connectivity efficiency between nodes s_i and s_j in a network. Hence, it is clear from

189 Eq. 6 that the meaning of network efficiency E_f is the average of node efficiency for all nodes in

190 a network. The value of E_f could range from zero to one, i.e., zero means no connectivity

191 between any two nodes in the network, whereas one means any two nodes are connected. This

192 specifies the lower and upper bounds for network connectivity.

193 Theoretically speaking, the connectivity of a topographical metro network could be affected

194 by failures both from metro stations (nodes) and from metro tunnels (links). In this paper, the

195 failure of metro stations is specifically considered but not the links. The key reason is that the

196 metro station is open to the public and thus vulnerable to attacks or other hazards. In addition,

197 the failure of a network node is often considered in L-space type topological graphs for

198 transportation networks (Yang et al., 2015; Zhang et al., 2011). The failure of a metro station

199 can be classified into two types. The first failure type occurs randomly and is caused possibly by

200 natural hazards, power and signal malfunction or even human errors. The probability of

201 occurrence of such a failure can be assumed to be the same for all stations in a network. This

202 assumption can be changed and varied values used without affecting the overall approach

203 although the computationally complexity increases. The second type of failure is of an

204 intentional nature as caused mainly on purpose by arson or terrorism. Usually, the most

205 important station in a large-scale network, e.g., a multi-line interchange, could be intentionally

206 targeted and disrupted. For topological analysis, the failure of a station can be modeled by

207 removing the node from the network. As for the random failure, the node is removed randomly

208 following a specific probability distribution function (Crucitti et al., 2004). As for the intentional

209 failure, assuming that attacks occur in the order of importance of the nodes, the nodes are

210 removed sequentially following a descending order of magnitude of the node degree k (Crucitti

211 et al., 2004).

212 Hence, the metric of robustness of a topological metro network can be quantitatively

213 described by the changed connectivity after the removal of a network node:

$$E'_f = \frac{1}{N'(N'-1)} \sum_{i \neq j} \frac{1}{d'_{ij}}$$

214 (7)

215 where N' is the number of nodes after the removal of failed nodes, and d'_{ij} is the newly calculated

216 path length between nodes s_i and s_j. Correspondingly, the vulnerability of the topological metro

217 network can be calculated by the decrease of connectivity due to the failure of nodes:

$$V = \Delta E_f = E_f - E'_f$$

218 (8)

219 As for a node removal strategy, only one node is removed at a time. Then the changed

220 connectivity E'_f and vulnerability V are calculated as the robustness and vulnerability of the

221 network, respectively. Hence, the magnitudes of robustness and vulnerability of a network

222 depend on the node that is disrupted. By examining all the nodes, one at a time, robustness and

223 vulnerability could indicate the order of importance of these metro stations for the network.

224 **2.3 Resilience of Metro Networks**

225 The resilience of a metro network as discussed in this paper is defined as the connectivity level

226 after the node disruption and the ability of rapid recovery of the connectivity to an acceptable

227 level with appropriate repair measures. The concept of the "*resilience triangle*" is often used for

228   infrastructure networks as proposed by <mark>Bruneau et al.</mark> (2003) to quantify the loss of resilience

229   after performance disruption. Figure 2 shows an example of such a resilience triangle shaded in

230   grey.   The vertical axis stands for the performance index $Q(t)$ of the network, while the

231   horizontal axis is the time t. The system performance is disrupted at time t_0. With particular

232   recovery measures applied in a time interval of t_h, the performance can be recovered to the

233   original level at time t_1 (i.e., $t_1=t_0+t_h$). Then, the resilience triangle is illustrated by the difference

234   between the area covered by constant Q_0 for the undisrupted system and the area covered by

235   varied $Q(t)$ for the disrupted system within time t_h. Furthermore, the area covered by $Q(t)$ for the

236   disrupted system in this period (yellow shaded in Figure 2) is an indicator for resilience of the

237   system subjected to the disruption at time t_0. Hence, on the basis of the resilience triangle,

238   Bocchini and Frangopol (2012) proposed a general metric of resilience for bridge network

239   infrastructure as:

$$R_e = \frac{\int_{t_0}^{t_0+t_h} Q(t)dt}{t_h Q_0}$$

240   (9)

241   The resilience index R_e is essentially the ratio of the area covered by the disrupted performance

242   curve $Q(t)$ (yellow shaded area in Figure 2) with respect to the area covered by the undisrupted

243   curve (constant Q_0 in the example of Figure 2) within the period of t_h. Hence, the metric of

244   resilience for a metro network can be represented by Eq. 9 with the performance $Q(t)$ referring to

245   the network efficiency E_f. Hence, the resilience index R_e can be expressed as:

$$R_e = \frac{\int_{t_0}^{t_0+t_h} \left[E_f(t) \right] dt}{t_h E_{f0}}$$

246   (10)

247   where $E_f(t)$ stands for the network efficiency at time t, and E_{f0} is the initial network efficiency for

248   the original metro network where no disruption has occurred.

11

249   When the connectivity of the network after removal of nodes needs to be recovered, a

250   sequential recovery strategy is usually assumed in the resilience analysis (Henry and Ramirez-

251   Marquez, 2012), i.e., only one metro station for one metro line could be recovered at a time. In a

252   large-scale metro network such as the Shanghai metro system, some of the metro stations are

253   multi-line exchange stations as shown in Figure 3a. When losing the functionality of such

254   stations, the recovery of connectivity for different metro lines in this station also needs to be

255   implemented sequentially. Specifically, if the exchange station connects m lines, there are m

256   stages in sequence to fully recover this station. Hence, in total, the number of optional sequences

257   is equal to $P(m,m)$ (i.e., m-permutations of m). As for the example shown in Figure 3b, in total,

258   there are six optional sequences to fully recover the three-line exchange station A (i.e., $6=3\times2\times1$).

259   A typical sequence is shown in Figure 3 with the first stage to recover Line 2 (Figure 3c), the

260   second to recover Line 1 (Figure 3d) and the last stage to recover Line 3 to its original state

261   (Figure 3a). Each recovery sequence corresponds to a specific resilience index R_e. Hence, an

262   optimal decision for a recovery strategy is to find the best sequence for recovery that maximizes

263   the value of R_e. Take the example of recovery of node A shown in Figure 3, the performance

264   recovery curves corresponding to the six optional recovery sequences are plotted in Figure 4.

265   Engineers thus could select sequence 5 as the optimal recovery strategy because it is associated

266   with the largest resilience index R_e. For the case of several damaged nodes the procedure applies

267   accordingly.

268   ***2.4 Disruption and Repair Costs for Decision Making***

269   The recovery of network connectivity is a primary goal for decision makers; however, disruption

270   and repair costs associated with recovery profiles a key criterion in decision making. Once the

271   recovery sequence is selected, the particulars of recovery plans, i.e., repair methods, equipment,

12

272   etc., affect the repair duration and subsequently the recovery cost. Generally, advanced

273   techniques for repair work require less time to complete recovery task, but at a greater cost.

274   Hence, a recovery cost analysis in terms of repair time duration helps to determine the optimized

275   cost of repair. Similar to other published resilience models, such as (Francis and Bekera, 2014),

276   the proposed model for the resilience of metro networks so far does not incorporate the cost-

277   benefit analysis directly in the decision-making process of selecting an appropriate repair

278   sequence. As an extension, this section proposes a general cost analysis model in conceptual

279   terms. Note that the cost analysis here is discussed based on the selected optimum repair

280   sequence by using the above resilience model. Following the basic model proposed by Henry

281   and Ramirez-Marquez (2012), the total cost C_{total} during the disruption and repair stages is

282   generally composed of two parts, namely the cost $C_{disruption}$ and the cost $C_{repairs}$, represented as:

$$C_{total} = C_{disruption} + C_{repair} \tag{11}$$

284   where the $C_{disruption}$ is referred to the cost or income loss due to the disruption of network

285   connectivity and the $C_{repairs}$ means the cost or investment for the repair works. Taking the flood-

286   induced failure of metro station as an example, the $C_{disruption}$ might include two major categories,

287   i.e., damaged but repairable equipment and damaged but non-repairable equipment, and income

288   loss due to closing of metro operations. Once a station is set as disrupted by flooding, the

289   equipment such as track barriers, escalator, signal board and etc., could be partially or totally

290   disabled. Later on, the control rooms and power plant rooms might also be affected due to

291   flooding. Furthermore, when the metro station is completely closed, loss in income from ticket

292   sales, the retails and other business around the metro stations comes on top. In addition, the

293   stocks or reputation of the metro company could be affected due to the disruptions. Details of

294   the above disruption cost are shown in Table 1. However, incorporating all the factors shown in

295 Table 1 for disruption cost $C_{disruption}$ requires data that are not available in some cases. For ease

296 of discussion, the cost analysis for $C_{disruption}$ in this paper includes mainly the income loss in the

297 ticket sales C_{ticket} ($C_{disruption} = C_{ticket}$ in this paper) which can be quantitatively evaluated. Some

298 other cost factors in Table 1 could be related qualitatively to the ticket income using perhaps

299 multiplication coefficients ($C_{others} = \lambda \times C_{ticket}$) as an example.

300   It is reasonable to assume that the income loss in metro ticket sales C_{ticket} is closely related to

301 the loss of network connectivity. In other words, the loss of system performance in terms of

302 network connectivity directly affects the passenger volume (*Vol*) of the network, in particular in

303 and around the disrupted stations. The passenger volume would further affect the income from

304 the ticket sales *I*. In that case, the ticket income cost C_{ticket} is assumed to have a positive

305 correlation with the loss of passenger volume by a linear model. As mentioned previously, the

306 disruption cost $C_{disruption}$ in this paper is assumed to be equal to ticket income loss C_{ticket}. Hence,

307 the $C_{disruption}$ is assumed as below:

$$C_{disruption} = C_{ticket} = \beta \cdot Vol_{Loss}$$

308   (12)

309 where Vol_{Loss} is the total loss of the passenger volume during the whole disruption period, and β

310 is the average metro ticket price of the network. Similar to the network connectivity, the

311 passenger volume *Vol* will experience a sharp reduction once a metro station is attacked or

312 removed from the network at time t_0. This reduction from the initial state of Vol_n to a disrupted

313 state Vol_d will be gradually recovered during the repair measures to the final recovered state at

314 time t_1. Hence the passenger volume $Vol(t)$ is also a function of time t between the failure time t_0

315 and the final recovered time t_1. Figure 5a shows two examples of linear and step functions of

316 recovery of passenger volume *Vol*. Corresponding to the passenger volume recovery, the

317 operation income is also recovered due to the increase of passenger volume, from the income I_d

318   under disruption to the fully recovered value of income I_n. This effect is captured by a

319   multiplication factor corresponding to the average ticket price β, see Eq. 12. Figure 5b shows the

320   two types of variation of operation income from I_d to I_n. In Figure 5, the shaded area

321   corresponds to the total passenger volume loss Vol_{Loss} (Figure 5a) and the total cost of operation

322   income loss $C_{disruption}$ (Figure 5b), respectively. If the recovery function of passenger volume Vol

323   is assumed to be linear, then the passenger volume loss can be represented as:

$$Vol_{Loss} = \frac{1}{2}\left(Vol_n - Vol_d\right)\left(t_1 - t_0\right)$$

324   (13a)

325   and the total cost of disruption of system performance $C_{disruption}$ is:

$$C_{disruption} = \frac{1}{2}\beta\left(Vol_n - Vol_d\right)\left(t_1 - t_0\right)$$

326   (13b)

327   This cost model does include indirect losses such as costs associated with longer travel times,

328   costs associated with increased demands on other transportation systems, costs attributed to

329   impacts on reputation and confidence in the system, etc. A complete accounting of all of these

330   effects requires simulating the dynamics of the system with the passengers and other

331   transportation modes.

332   Given an existing large-scale metro network, the average ticket price β and the initial

333   passenger volume Vol_n are known. After a node failure at time t_0, the disrupted passenger

334   volume Vol_d can also be predetermined for the disrupted system. Hence, the only variable in Eq.

335   13b that governs the cost $C_{disruption}$ is the time t_1 that is needed to recover the system to its initial

336   state, i.e., removed nodes are all repaired. Note that the time t_1 is positively correlated with the

337   cost $C_{disruption}$, e.g., a positive linear relationship could be found in the above example of linear

338   model (Eq. 13). It is obvious that the longer the repair works last, the greater the cost is.

339　　　The cost for the implementation of repair measures C_{repair} is determined by solving a typical

340　　time-cost trade-off problem within the discipline of engineering economics (Golzarpoor, 2012;

341　　Hegazy, 1999; Liu et al., 1995). The total cost of repair works consists of the direct cost and the

342　　indirect cost, as shown in Figure 6. The direct cost is related to the salary of workers,

343　　consumption of engineering materials, rental of the engineering machinery etc. Some typical

344　　direct cost is shown in Table 1. For a certain repair project, shortening the repair duration t can

345　　be achieved by an increase of salary, the use of high quality materials, and more machinery.

346　　Hence, the direct cost is believed to have a negative correlation with the repair time duration t as

347　　shown by the red dashed line in Figure 6. The indirect cost is caused by social related factors

348　　(also shown in Table 1), which is believed to have a positive correlation with the time duration t,

349　　as indicated by the blue dashed line in Figure 6. It is widely recognized that the detailed

350　　evaluation of direct and indirect cost is quite complicated and specifically case-oriented

351　　(Golzarpoor, 2012). Hence, the cost C_{repair} is represented by a non-monotonic and nonlinear

352　　function of repair duration t_1 without loss of generality, as shown in Figure 13, marked as black

353　　solid line, from which an optimum value of t_1 that minimizes the C_{repair} can be found (point A in

354　　Figure 6).

355　　　Hence, by substituting the above expressions for $C_{disruption}$ and C_{repair} into Eq. 11, the total cost

356　　C_{total} becomes:

$$C_{total} = \frac{1}{2}\beta\left(Vol_n - Vol_d\right)\left(t_1 - t_0\right) + C_{repair}(t_1)$$

357　　(14a)

358　　　Figure 7 shows a graphical representation of Eq. 14a by plotting the total cost C_{total} against the

359　　repair duration t_1. Again, for a particular large-scale metro network under a specific case of

360　　disruption and recovery, the dominant variable in Eq. 14a is the repair duration t_1. Similar to the

361　　non-monotonic function of C_{repair}, the total cost C_{total} is also a non-monotonic function of time t_1.

16

362   To minimize C_{total} is again a typical time-cost trade-off problem. Interestingly, it is not always

363   the case that a shorter recovery is associated with a smaller total cost. The optimum value of t_1

364   that minimizes the total cost of recovery needs to be determined by solving the time-cost trade-

365   off problem illustrated in Figure 7 with point B being the solution. Since the total cost includes

366   the operation income loss (first term on the right-hand side of Eq. 14a), the optimum value of t_1

367   is smaller than the value of time t that minimizes C_{repair}, i.e., $t_{1,\,B}$ in Figure 7 is smaller than $t_{1,\,A}$

368   in Figure 6.

369   If the disruption is quite serious, the duration of full recovery can take several years or even

370   longer. For example, the reported disruption of metro lines in Shanghai due to deformational

371   performance took almost six years to be fully recovered (Huang and Zhang, 2016) and the

372   disruption of metro lines in St. Petersburg due to seepage in tunnels takes almost eight years of

373   recovery (Ryumin, 2004). In those cases, the factor of time-value of money should be included

374   in the cost analysis at the present time. In the simplest model for time-value of money a constant

375   discount rate i is assumed (Brigham and Ehrhardt, 2002), and Eq. 14a is modified to:

$$C_{total,PV} = \left[\frac{1}{2} \beta \left(Vol_n - Vol_d \right) \left(t_1 - t_0 \right) + C_{repair} \left(t_1 \right) \right] \cdot \frac{1}{\left(1 + i \right)^{t_1}}$$

376   (14b)

377   It is clear from Eq. 14b that the total cost with full recovery at time t_1 (present value equal to

378   the total cost at time t_1, i.e., $C_{total,\,PV}$) is less than the value of money at present (C_{total}). A

379   generalized illustration of the comparison between $C_{total,\,PV}$ and C_{total} is also plotted in Figure 7.

380   The corresponding optimum value of t_1 might move forward due to the effect of time value of

381   money as the point D shown in Figure 7. Owner or practitioner with the responsibility for the

382   repair and maintenance works of large-scale metro networks should undertake such cost analysis.

383   After determining the optimal repair sequence by the resilience analysis model as shown in

384 <mark>Figure 4, the optimal repair duration for each station could be obtained from the above cost</mark>

385 <mark>analysis. Therefore, the best recovery strategy due to the disruption can be achieved both with</mark>

386 <mark>the best recovery sequence and duration.</mark> At the present stage, it should be noted that the detailed

387 evaluation for each parameter in Eq. 14b is limited to typical scenario where both the data from

388 disruption and recovery could be collected.

3. Application: Shanghai Metro System

390   The Shanghai metro system now is the longest metro network system in the world by the

391 route length. Up to December 31, 2015, the total length of the 14 Shanghai metro lines in

392 operation was 617km with 303 metro stations. These numbers exclude the operating magnetic

393 train line that only has a departure station and an arrival station. The planned and being-

394 constructed metro lines and stations are also excluded from these values. For planning reasons,

395 Metro lines 3 and 4 in Shanghai partially share the same line and metro stations along the line.

396 Those shared metro stations and lines are considered only once in building the network as

397 described in this paper. The necessity of a detailed resilience analysis for such a huge-scaled

398 network is quite obvious from this perspective.

3.1 Topological Characteristics of the Shanghai Metro

400   A typical L-space topological network representing the Shanghai metro system is built and

401 plotted in Figure 8. The nodes in Figure 8 represent the metro stations, and the links between

402 nodes are the metro lines. The correlation matrix A is built for all 303 stations in this network,

403 $A=[a_{ij}]_{303\times303}$. Based on the correlation matrix A, the characteristics of the metro network, i.e.,

404 average degree k^*, characteristic path length L and network diameter D, are calculated by using

405 the algorithm proposed by Floyd (1962). Table 2 displays these typical characteristics for the

406 Shanghai metro network.

407   The average node degree k^* is equal to 2.31, which indicates that every station is connected to

408   2.31 other stations on average. Note that a node degree k equal to one refers to an endpoint of a

409   single line. A k equal to two characterizes an intermediate normal station where only one metro

410   line passes through. A value of k larger than two indicates an exchange station for at least two

411   lines in a metro system. Figure 9a shows the histogram for the distribution of node degrees for

412   the 303 stations, represented by the solid black column. In total, about 76% of the metro stations

413   are normal stations passed by one metro line. The remaining 24%, i.e., 52 stations, are multi-line

414   exchange stations. For comparison, the distribution of node degrees for the Shanghai metro

415   system from 2010 is plotted in the grey column in Figure 9a based on data extracted from Zhang

416   et al. (2011). It can be seen that the relative frequency for the node degree equal to 2 is smaller

417   in 2015, while the values for node degree equal to 4, 5 or 6 are larger. Furthermore, the largest

418   value of node degree k is equal to 8, which means that four metro lines pass through this station.

419   The largest k in the year of 2010 is equal to 7. This indicates the fast development of the

420   Shanghai metro network during these five years from 2010 to 2015.

421   Figure 9b shows a plot with logarithmically scaled axes for both the node degree k and the

422   relative frequency $p(k)$, corresponding to Figure 9a for the case of 2015. The plot provides some

423   indication that the relationship between the logarithm of relative frequency $p(k)$ and the

424   logarithm of node degree k can be approximated in a linear manner. This corresponds to a power

425   curve for the distribution of the node degree k. Linear regression yields the parameters α=3.858

426   and γ=3.525. Hence, it is indicated that the Shanghai metro network is a scale-free network,

427   which corresponds to robustness of the network for random failure but vulnerability of the

428   network for an intentional failure (Albert et al., 2000; Crucitti et al., 2003; Crucitti et al., 2004).

429   The characteristic path length L shown in Table 2 is equal to 14.87, which indicates that the

430   shortest path between any two stations in the network needs to pass 14.87 stations from an

431   average perspective. The network diameter D is equal to 41, which stands for the longest metro

432   line with 41 metro stations. The calculated network cluster coefficient C is 0.0082. Table 2 also

433   displays the calculated path length limit of 6.82 ($\ln N / \ln k^*$) and the limit for the network cluster

434   coefficient C as 0.0076 for concluding whether the network is a small-world network or not, see

435   Eq. 4. Both criteria indicate that the Shanghai metro network is a small-world network. From

436   the definition of small-world given by Milgram (1967), the Shanghai metro network is proved to

437   have an intensive connectivity locally and a good quality of operation for the whole network.

3.2 Robustness and Vulnerability Evaluation of Shanghai Metro

439   The initial network connectivity E_f without any failure is calculated by using Eq. 6, where the

440   node number N is equal to 303 and the path length d_{ij} for all pair nodes in network is calculated

441   by using the Floyd algorithm (Floyd, 1962). The calculated E_f is equal to 0.0994. After the

442   disrupted node is removed, the similar procedure of calculation could be repeated for a disrupted

443   network as described above. The robustness of the Shanghai metro is calculated for both types

444   of failure scenarios, random failure and intentional failure, corresponding to the respective node

445   removal strategies. For random failure, stations are removed randomly following a discrete

446   uniform distribution over the stations. The network connectivity $E_{f,random}$ is calculated using Eqs.

447   6 and 7 after each station removal. For intentional failure, the stations are removed in the order

448   of descending node degree. The network connectivity $E_{f,intention}$ is calculated after each station

449   removal.

450   Figure 10 shows the calculated $E_{f,random}$ (green line with solid triangle) and $E_{f,intention}$ (blue line

451   with solid rectangle) against the fraction of removed stations in the network. The constant

452   dashed line stands for the calculated initial network connectivity E_f (i.e., 0.0994) without failure

453   of any station. It is observed that the decrease of $E_{f,intention}$ with the growing fraction of removed

454   nodes experiences two distinct stages. First there is a sharp decrease at the beginning followed by

455   a more gentle decrease once a number of stations have already failed. By drawing two extension

456   lines (black dash line in Figure 10) along these two distinct stages, the intersection of these two

457   lines could be regarded as the inflection point. The inflection point shown in Figure 10 is around

458   the fraction of removed nodes equal to 0.10. This fraction of removed nodes is approximately

459   the fraction of nodes in the network with node degree greater than 3, see Figure 9a. This is a

460   clear indication for the importance of those multi-line exchange stations for the connectivity of

461   the metro network. Similarly, the decrease of $E_{f,random}$ also shows these two stages, as well, with

462   the inflection point at around 0.24. The inflection point for random attack is greatly moving to

463   the right side of the inflection point for intentional attack. It clearly shows that the robustness of

464   the metro network under the condition of random attack is much better than the robustness under

465   the condition of intentional attack. But the curve for $E_{f,random}$ is less sharp compared to the curve

466   for $E_{f,intention}$ due to the large value at the inflection point for random failure. Hence, the

467   Shanghai metro network when subjected to the random failure of stations is more robust than the

468   network when subjected to intentional attacks. This result is consistent with the general

469   conclusions for scale-free networks and supports our hypothesis that the Shanghai metro is a

470   scale-free network. Further, when the fraction of removed stations is greater than 35%, $E_{f,intention}$

471   is slightly larger than $E_{f,random}$ since the random removal leaves some exchange stations for

472   removal in later stages causing a slightly stronger decrease of connectivity in those stages.

473   For comparison, the results based on the data of the network in 2010 are also represented in

474   Figure 10. The grey line with hollow triangles illustrates the random removal strategy, while the

475   red line with hollow rectangles indicates the intentional removal strategy. By comparing the

476   results for 2015 and 2010, both the $E_{f,random}$ and $E_{f,intention}$ for 2015 are slightly larger than those

477   for 2010, especially when the fraction of removed nodes is small. This suggests that the

478   robustness, in particular at the beginning of removal stages, has been increased by the five-year

479   development of the metro network from 2010 to 2015. Furthermore, the network connectivity in

480   2010 under intentional removal would be close to zero when 40% of stations are removed, which

481   shows high vulnerability of the network. This issue has been resolved by 2015.

482   The vulnerability of the initial network subjected to only one node removal is calculated by

483   using Eq. 8 for all the 303 nodes. The ten most critical stations, identified by the largest V

484   calculated from Eq. 8, are displayed in Table 3. The *Caoyang Road station* is ranked most

485   critical station in the network. If this station is removed, the connectivity would be reduced by

486   0.0073, which is about 7.4% of the value of original connectivity E_f(0.0994). Inspecting the ten

487   most critical stations in Table 3 it appears that these stations do not necessarily have a large node

488   degree k (last column in Table 3). The stations with node degree equal to six are not ranked in

489   the top ten most critical stations. Apart from the *Century Ave station* with k equal to 8, all the

490   other stations have a node degree k of 5 or less. This result shows that the vulnerability of a

491   network due to one-node removal is not significantly correlated with the node degree k (Hu,

492   2007).

493   The specific locations of the ten most critical stations are marked in the network map in

494   Figure 8. Analyzing this map it becomes obvious that most of the critical nodes are located in a

495   position where the node is the only connection between the suburban and the downtown area.

496   Furthermore, the suburb metro lines still have a significant number of stations beyond the critical

497   stations. Once such a critical node is removed, the entire connection between downtown and the

498 respective suburb would be completely disrupted. This is the key reason for the vulnerability of

499 the Shanghai metro. As a conclusion, a new circle line should be implemented into the network

500 to remove this criticality. On the other hand, the nodes with a node degree k equal to 6 are

501 mostly located in the downtown area. Since the network in the downtown area is much denser

502 than that in the suburban area, even removal of such node with large k does not affect the

503 network connectivity badly. Once such node is removed, there are still sufficient options for

504 connecting through alternative lines.

3.3 Resilience Evaluation of Shanghai Metro

506   It is clear from Figure 4 that the resilience of a network highly depends on the recovery

507 strategy, e.g., sequence of recovery for multiple disrupted nodes and sequence of recovery for

508 multiple lines in an exchange station. Furthermore, repair duration should be optimized on the

509 basis of minimizing the disruption and repair costs. The philosophy behind the recovery strategy

510 for a disrupted metro system is first to select the best recovery sequence either for an exchange

511 station or for multiple stations and second to select the best repair duration considering both the

512 disruption and repair cost. In this regard, the following section shows an example of three

513 typical cases of the resilience analysis of the Shanghai metro network: Case 1 is to obtain the

514 best recovery sequence for a disrupted exchange station; Case 2 is to obtain the best recovery

515 sequence for multiple disrupted stations; and Case 3 is to obtain the best repair duration for

516 rebuilding a disrupted metro station.

Case 1: Recovery sequence given disruption of one multi-line exchange station

518   This analysis concentrates on the station with the largest node degree in the network, i.e.

519 *Century Ave station* connecting four metro lines, namely line 2, 4, 6 and 9, leading to a node

520 degree of 8. The robustness analysis indicated that the vulnerability of the network is

521   significantly determined by possible disruption of this station. That is, this station plays an

522   important role for the connectivity of the network, see Figure 11. High resilience is thus required

523   for this station. The key question is the decision for the best recovery strategy. There are 24

524   possible recovery sequences to fully recover all four lines in this station, i.e., 24 = $P(4, 4)$ =

525   4×3×2×1. Each sequence corresponds to a specific resilience index R_e representing the recovery

526   of network connectivity. A decision has to be made for that recovery sequence that maximizes

527   the value of R_e among the 24 choices. For carrying out the resilience analysis, we assume that

528   the recovery time for each line in this station is the same no matter what kind of recovery

529   measures are applied. On this basis, the difference of R_e between the possible sequences is

530   solely affected by the sequence of recovering metro lines in this station and not by any other

531   factors. Subsequently, the recovery sequences are denoted using the metro line numbers, such as

532   2-6-9-4 indicating that first line 2 is recovered, then line 6 and so on.

533   The resilience index R_e is calculated, using Eq. 10, for the 24 possible recovery sequences.

534   Considering the recovery sequence 2-6-9-4 as an example, the calculated initial network

535   connectivity is equal to 0.0994, and the network connectivity after the disruption of the station is

536   0.0932. After recovery according to the sequence 2-6-9-4, the network connectivity is gradually

537   increased from 0.0932 to 0.0953 (Line 2 is recovered), to 0.0973 (Lines 2 and 6 are recovered),

538   to 0.0985 (Lines 2, 6 and 9 are recovered), and to 0.0994 (fully recovered for Lines 2, 6, 9 and 4).

539   Hence, by using Eq. 10, the resilience index R_e is calculated to be 0.974, i.e., 0.974 = 0.5 ×

540   (0.0932 + 2 × 0.0953 + 2 × 0.0973 + 2 × 0.0985 + 2 × 0.0994) × 4 / (4×0.0994). The results are

541   listed in Table 4. The largest R_e shown in Table 4 is equal to 0.974, which is produced by the

542   recovery sequence 2-6-9-4. It indicates that if *Century Ave station* is totally disrupted, the first

543   metro line to be recovered is line 2, followed by line 6, then line 9, and line 4. On the other hand,

544   the smallest R_e is obtained as 0.962 for the recovery sequence of 9-4-6-2. The curves illustrating

545   the change of the network efficiency over these two recovery sequences are plotted in Figure 12.

546   The black line with solid squares reflects the recovery sequence 2-6-9-4, while the grey line with

547   hollow circles represents the recovery sequence 9-4-6-2. ==Stage zero stands for a metro network==

548   ==in its normal state without any disruption. The initial network efficiency as calculated in the==

549   ==robustness analysis is about 0.0994.== Stage 1 stands for the removal of the station causing the

550   sharp reduction of network efficiency to 0.0932. After four stages, the station is fully recovered

551   with a network efficiency restored to 0.0994 corresponding to the initial or normal condition. It

552   is quite obvious from Figure 12 that after each intermediate recovery stage, i.e., stage 2-4, the

553   network efficiency for sequence 2-6-9-4 is larger than that for sequence 9-4-6-2. Hence, the

554   resilience loss triangle for sequence 2-6-9-4 is much smaller than that for sequence 9-4-6-2. The

555   difference between the resilience triangles is shaded in red color in Figure 12. It indicates the

556   extent to which resilience of this station is influenced by decision margins regarding the recovery

557   sequence and that the sequence 2-6-9-4 is the best choice. Following this principle, the best

558   recovery strategy for each of the 52 exchange stations can be determined. Table 5 shows the best

559   recovery strategy for each exchange station in Shanghai based on the resilience analysis. This

560   result may be helpful for decision making when any of the stations is affected and waiting for

561   recovery.

562   *Case 2: Recovery sequence given disruption of multiple stations*

563   For the case of multi-station disruption, the removal of four nodes at once is taken as an

564   example. Two typical sub-cases are discussed: (I) with different node degree k values for the

565   four nodes, and (II) with the same node degree k for the four nodes. For multiple stations, in

566   order to show the effect of recovery sequence of different stations clearly, the recovery sequence

567   of metro lines for an exchange station discussed previously is not considered. In other words,

568   any of the removed stations is fully recovered only by one stage without considering the

569   sequence of recovering different lines.

570   For Sub-case I, the *Century Ave station* (node 43), *Peoples' Square station* (node 13),

571   *Oriental Sports Center station* (node 133) and *Shanghai railway station* (node 16) are selected

572   with their corresponding node degree k equal to 8, 6, 5 and 4, respectively. Again, there are 24

573   possible recovery sequences, i.e., 24 = $P(4, 4)$. The recovery sequences are denoted using the

574   station numbers, i.e. 43-13-133-16 for recovery in the order of stations as named above. The

575   resilience index R_e for each of the recovery sequences is calculated by Eq. 10. Hence, there are

576   24 calculated index values R_e as shown in Table 6. The maximum value of R_e is calculated based

577   on the sequence 16-43-133-13 which is the best choice according to the resilience measure. It is

578   quite interesting that the best recovery sequence is not based on the descending order of the node

579   degree k as 43-13-133-16. Instead, the best recovery sequence reflects the order of nodes ranked

580   according to their criticality for network vulnerability based on the robustness analysis. The key

581   criterion is the contribution of node to the network connectivity, and hence to the network

582   efficiency E_f, rather than the node degree k. The minimum value of the R_e is obtained as 0.885

583   for sequence 13-133-43-16, which is 5% less than the maximum value of R_e under the sequence

584   16-43-133-13. The difference of the index R_e between these two sequences corresponds to the

585   difference in the resilience loss triangle produced by the curves of recovered network efficiency

586   along the specific recovery sequence, as shown in Figure 13.

587   For Sub-case II with four removed nodes having the same node degree k value, *Xu Jia Hui*

588   *station* (node 8), *Peoples' Square station* (node 13), *Han Zhong Road station* (node 15) and *West*

589   *Nanjing Road* (node 39) are selected for analysis. In this example node degree k is equal to 6 for

590   each of these stations. Again, 24 possible recovery sequences are evaluated in the resilience

591   analysis. The respective values R_e calculated from Eq. 13 are listed in Table 7. It is interesting

592   that the values of R_e for different recovery sequences are quite close to one another. Hence, in

593   the present case the effect of the sequence of recovery for the nodes considered is not significant

594   for the resilience of the metro network. However, it should not be concluded, in general, that

595   this effect is caused by the same node degree. The reason is rather the similar contribution of

596   these nodes to the network connectivity, as the calculated robustness of the network connectivity

597   after the disruption of each node is almost the same among these four nodes.

598   ***Case 3: Recovery cost to rebuild a disrupted metro station***

599   In this hypothetical example, a metro station is disrupted completely at time t_0 and requires

600   rebuilding of the damaged station. For ease of discussion, t_0 is assumed to be zero. In addition,

601   time-value of money is not considered in this example for simplicity. During the repair

602   procedure, the metro station is closed to the public. As mentioned previously, the disruption cost

603   in the recovery stage is assumed to only include the income loss related to metro tickets. From

604   the statistics of the Shanghai metro, the daily passenger flow volume is more than 10 million.

605   Hence, the disruption of one station among the 303 stations of the whole network is assumed to

606   lead in a loss of about 40 thousand passengers flow volume every day. The ticket price of

607   Shanghai metro is about 4 RMB on average. For this case, from Eq. 13b, the disruption cost

608   during the recovery procedure can be calculated as below:

$$C_{disruption} = \frac{1}{2} \times 4 \times 40000 \left(t_1 - t_0 \right) \tag{15}$$

610   where t_1 is the recovered time moment that is unknown and needs to be optimized and t_0 is equal

611   to zero that is assumed in this example.

612   The rebuilding of a metro station requires several stages in sequence, including the site

613   investigation, construction of a pile foundation of underground structures, construction of a soil

614   retaining system, soil excavation with construction of supports and dewatering, and construction

615   of underground structures of the metro station. From personal communication with the managers

616   in charge of design, construction and operation, Table 8 shows a typical example of repair

617   options associated with the direct cost and duration for rebuilding one typical metro station in

618   Shanghai. It is quite obvious from direct cost perspectives that the shorter the repair duration,

619   the higher the cost. Solving such a typical time-cost tradeoff requires the use of linear and integer

620   programming (LP/IP) models, such as Liu et al. (1995). Table 9 shows the calculated results of

621   repair duration and associated direct cost of construction. The indirect cost is assumed, in this

622   example, to be equal to 100 thousands RMB per day. Hence, the total indirect cost can also be

623   calculated based on the calculated duration, as shown in Table 9. Figure 14a shows the

624   calculated direct cost, indirect cost and the repair cost against the repair duration, respectively

625   (solid circles for C_{repair}, hollow triangles for direct cost and hollow rectangles for indirect cost).

626   It is observed from Figure 14a that the optimized repair duration based on repair cost is around

627   455 days. Corresponding to this calculated repair duration, the disruption cost in terms of the

628   ticket income loss can be derived from Eq. 15, as displayed in Table 9. Hence, the total cost

629   C_{total} both including $C_{disruption}$ and C_{repair} can be obtained as shown in Figure 14b (solid circles for

630   C_{total}, hollow circles for C_{repair} and hollow rectangles for $C_{disruption}$). The optimized repair duration

631   after incorporating the income loss is about 450 days, which is less than the optimized duration

632   considering only repair cost. This finding is reasonable, as the income loss will continue to

633   increase when the repair work is not finished. In this example, the disruption cost only includes

634   the ticket income loss, resulting in a five-day decrease of the optimized duration. Although the

635 number of days in this case is small, the best repair duration might be reduced further as other

636 cost elements of disruption are considered. If the other disruption cost as shown in Table 1 is

637 considered to be proportional to the ticket income loss, i.e., $\lambda = (C_{disruption}-C_{ticket})/C_{ticket}$, Figure

638 14c has illustrated the effect of parameter λ on the optimized repair duration days. It is clear that

639 as the λ becomes larger, i.e., that is to say, the other disruption cost increases, the optimized

640 repair duration days would be greatly reduced. It is consistent with the engineering practice that

641 if the disruption cost is invaluable or social effect of the metro accident is unacceptable, the best

642 repair strategy should be as fast as possible.

4. Conclusions

644 In view of the ever-increasing concerns on the safety of metro systems, a general framework

645 for resilience analysis of large-scale metro networks is presented in this paper. This framework

646 includes the topological mapping of a metro network and the quantitative evaluation of

647 robustness and vulnerability as a basis to quantify resilience and to derive decisions regarding the

648 most resilient recovery strategy. The analysis framework captures both random failure and

649 intentional attacks. The node connectivity, defined by the network efficiency E_f, is regarded to

650 be the key performance criterion of a metro network. The proposed resilience assessment

651 framework is applied to the Shanghai metro network, which is one of the largest metro networks

652 in the world. The following conclusions are drawn from analysis.

653 1) The Shanghai metro system is a typical small-world and scale-free network under the

654 topological L-space. It has strong connectivity locally and a good quality of operation for the

655 whole network. The characteristics of a scale-free network, i.e., strong robustness of network

656 connectivity under random attacks; but serious vulnerability under intentional attacks, has

657   been quantitatively validated by the proposed analysis model for evaluation of robustness and

658   vulnerability for the Shanghai metro network.

659   2) The vulnerability of the metro network is quantified by the network global efficiency when

660   removing disrupted nodes. However, the magnitude of vulnerability when removing a

661   disrupted node does not only depend on the degree of this node, but also on the contribution

662   of this node to the global network efficiency. That is, the most critical node for vulnerability

663   of a metro network, i.e., *Caoyang Road station* in the Shanghai case, might not be the node

664   with the largest node degree k but is the node with the largest contribution to the network

665   connectivity.

666   3) The recovery strategy in terms of recovery sequence for the case of recovering a multi-line

667   exchange station and the case of recovering multi stations can be derived with the concept of

668   minimizing the area of the resilience triangle based on the performance evolution curves.

669   Similar to the vulnerability analysis, the optimum recovery sequence depends not only on the

670   degree of the recovered nodes but also on the contribution of the recovered nodes to the

671   network connectivity. Given an optimized recovery sequence, the recovery time duration can

672   be optimized by minimizing the cost including the disruption and repair cost for the disrupted

673   metro system. The total cost is a non-monotonic function of repair duration time t_1, with its

674   local minimum of cost indicating the best choice for recovery measures at the associated

675   optimum time t_1.

676   It should be specifically noted that the topology of the metro network discussed in this paper

677 is under the assumption of an undirected and unweighted network. Although this simplification

678 is widely accepted for basic understandings of a large-scale infrastructure network, some of the

679 practical factors are not included in this model, such as the physical length of tunnels between

680   stations, the time and route for exchanging metro lines, the volume for different metro lines and

681   also political factors. Those weights on the importance of nodes and links in the metro network

682   could be explored in future studies.

683   **5. Acknowledgement**

688   **6. Notations**

689	G	Topological vector for metro network
690	S	Node set of a metro network
691	s_i	Node in a metro network
692	N	Node number in a metro network
693	E	Link set of a metro network
694	e_{ij}	Link between node s_i and s_j in a network
695	A	Correlation matrix for a network
696	a_{ij}	Correlation between node s_i and node s_j
697	d_{ij}	Path length between node s_i and s_j
698	L	Characteristic path length of a network
699	D	Diameter of a network
700	C_i	Clustering coefficient for a node in a network
701	C	Clustering coefficient of a network
702	$P(k)$	Distribution of node degree for a network
703	E_f	Network efficiency
704	V	Vulnerability of topological metro network
705	$Q(t)$	System performance of a metro network at time t
706	t_0	Time moment when failure or attacks occur to the metro network
707	t_1	Time moment when the metro network is fully recovered from a disruption

708	t_h	Time duration from the disruption moment t_0 to the recovered moment t_1
709	R_e	Resilience index for metro network
710	C_{total}	Cost during the system disruption
711	$C_{total, PV}$	Present value equal to the total cost at time of recovery
712	$C_{disruption}$	Cost referred to the loss of system performance
713	C_{ticket}	Cost referred to the income loss of metro ticket
714	Vol	Passenger volume of the metro network
715	Vol_n	Initial passenger volume of a metro network in normal condition
716	Vol_d	Reduced passenger volume of a metro network after disruption
717	Vol_{Loss}	Total loss of the passenger volume during the disruption
718	C_{repair}	Cost related to the implementation of repair measures

719 **7. References**

720 Albert, R., Jeon, H., Barabasi, A.L., 2000. Error and attack tolerance of complex networks.
721   Nature 406, 378-382.

722 Ayyub, B.M., 2014. Systems resilience for multihazard environments: definition, metrics, and
723   valuation for decision making. Risk Analysis 34, 340-355.

724 Ayyub, B.M., 2015. Practical Resilience Metrics for Planning, Design, and Decision Making.
725   ASCE-ASME Journal of Risk and Uncertainty in Engineering Systems, Part A: Civil
726   Engineering 1, 04015008.

727 Barabasi, A.L., Albert, R., 1999. Emergence of scaling in random networks. Science 286, 509-
728   512.

729 Bocchini, P., Frangopol, D.M., 2012. Restoration of Bridge Networks after an Earthquake:
730   Multicriteria Intervention Optimization. Earthquake Spectra 28, 427-455.

731 Brigham, E.F., Ehrhardt, M.C., 2002. Financial management theory and practice. Implementing
732   Integrated Water Resources Management in Central Asia 1, 3-21.

733 Bruneau, M., Chang, S.E., Eguchi, R.T., Lee, G.C., O'Rourke, T.D., Reinhorn, A.M., Shinozuka,
734   M., Tierney, K., Wallace, W.A., von Winterfeldt, D., 2003. A framework to quantitatively
735   assess and enhance the seismic resilience of communities. Earthquake Spectra 19, 733-752.

736 Crucitti, P., Latora, V., Marchiori, M., Rapisarda, A., 2003. Efficiency of scale-free networks:
737   error and attack tolerance. Physica a-Statistical Mechanics and Its Applications 320, 622-642.

738   Crucitti, P., Latora, V., Marchiori, M., Rapisarda, A., 2004. Error and attacktolerance of complex
739   networks. Nature 340, 388-394.

740   Derrible, S., Kennedy, C., 2010. The complexity and robustness of metro networks. Physica a-
741   Statistical Mechanics and Its Applications 389, 3678-3691.

742   Dong, Y., Frangopol, D.M., 2015. Risk and resilience assessment of bridges under mainshock
743   and aftershocks incorporating uncertainties. Engineering Structures 83, 198-208.

744   Floyd, R.W., 1962. Algorithm 97 (Shortest Path). Communications of the Acm 5, 345-345.

745   Francis, R., Bekera, B., 2014. A metric and frameworks for resilience analysis of engineered and
746   infrastructure systems. Reliability Engineering & System Safety 121, 90-103.

747   Frangopol, D.M., Soliman, M., 2015. Life-cycle of structural systems: Recent achievements and
748   future directions, 4th International Symposium on Life-Cycle Civil Engineering, IALCCE
749   2014, November 16, 2014 - November 19, 2014. CRC Press/Balkema, Tokyo, Japan, pp. 3-
750   17.

751   Golzarpoor, B., 2012. Time-Cost Optimization of Large-Scale Construction Projects Using
752   Constraint Programming. University of Waterloo, Waterloo, Canada.

753   Hashimoto, T., Stedinger, J.R., Loucks, D.P., 1982. Reliability, resiliency, and vulnerability
754   criteria for water resource system performance evaluation. Water Resources Research 18, 14-
755   20.

756   Hegazy, T., 1999. Optimization of construction time-cost trade-off analysis using genetic
757   algorithms. Revue Canadienne De Génie Civil 26, 685-697.

758   Henry, D., Ramirez-Marquez, J.E., 2012. Generic metrics and quantitative approaches for system
759   resilience as a function of time. Reliability Engineering & System Safety 99, 114-122.

760   Holling, C.S., 1973. Resilience and stability of ecological systems. Annual review of ecology
761   and systematics, 1-23.

762   Hu, L.L., 2007. The relationship between construction time and construction cost. Railway
763   Engineering Cost Management 3, 15-17 (in Chinese).

764   Huang, H.-W., Zhang, D.-M., 2016. Resilience analysis of shield tunnel lining under extreme
765   surcharge: Characterization and field application. Tunnel. Under. Space. Tech. 51, 301-312.

766   Latora, V., Marchiori, M., 2001. Efficient behavior of small-world networks. Physical Review
767   Letters 87, 4.

768   Liu, L., Burns, S.A., Feng, C.W., 1995. Construction Time-Cost Trade-Off Analysis Using LP/IP
769   Hybrid Method. Journal of Construction Engineering & Management 121, 446-454.

770   Milgram, S., 1967. The small world problem. Psychology 1, 60-67.

771   Mu, X.Q., 2011. Two subway trains collide in Shanghai, over 270 injured, Xinhuanet.
772   Xinhuanews, Beijing.

773   PPD-21, 2013. Critical infrastructure security and resilience. Directive Presidential Policy-21.

774   Ryumin, A.N., 2004. On hydrogeomechanical causes of accident in the subway of Saint
775   Petersburg. Journal of Mining Science 40, 11-23.

776   von Ferber, C., Holovatch, T., Holovatch, Y., Palchykov, V., 2009. Public transport networks:
777   empirical analysis and modeling. European Physical Journal B 68, 261-275.

778   Watts, D.J., Strogatz, S.H., 1998. Collective dynamics of 'small-world'networks. Nature 393,
779   440-442.

780   Yang, Y., Liu, Y., Zhou, M., Li, F., Sun, C., 2015. Robustness assessment of urban rail transit
781   based on complex network theory: A case study of the Beijing Subway. Safety Science 79,
782   149-162.

783   Zhan, F.B., Noon, C.E., 1998. Shortest path algorithms: an evaluation using real road networks.
784   Transportation science 32: 65-73.

785   Zhang, J., Zhao, M., Liu, H., Xu, X., 2013. Networked characteristics of the urban rail transit
786   networks. Physica A: Statistical Mechanics and its Applications 392, 1538-1546.

787   Zhang, J.H., Xu, X.M., Hong, L., Wang, S.L., Fei, Q., 2011. Networked analysis of the Shanghai
788   subway network, in China. Physica a-Statistical Mechanics and Its Applications 390, 4562-
789   4570.

790   Zhang, W., Wang, N., 2016. Resilience-based risk mitigation for road networks. Structural
791   Safety 62, 57-65.

792

794

825   Figure 10 Robustness of the Shanghai metro network under different node removal type (Data

826   for year of 2010 is extracted from Zhang et al., (2011))

827   Figure 11 The effect of failure of Century Ave station on the surrounding network

828   Figure 12 Comparison of change of network efficiency under two different recovery sequences

829   for recovering a multi-line exchange station.

830   Figure 13 Comparison of change of network efficiency under two different recovery sequences

831   for recovering a multi-line exchange station.

832   Figure 14 Time-cost trade-off analysis for rebuilding a metro station: a) time-cost for repair cost;

833   b) time-cost for total cost including disruption cost and repair cost; and c) effect of other

834   disruption cost on the optimized repair duration days.

835

836

838   Table 1 Cost produced due to disruption of metro station

Cost Category		Content
Disruption cost	Damaged equipment	track track barrier escalator signal board ticket barrier air-conditioning system ventilation system
	Abandonment of facility	managing control room power plant room ventilation room signal system room escape shaft
	Income loss	metro ticket retail mall rental real estate
	Stocks	stocks
Repair Cost	Direct cost	salary of workers monitoring and inspection before repair site investigation construction materials rental of engineering machinery purchase of power, ventilation and signal system
	Indirect cost	time value social impact

839

841

842   Table 2 Characteristic indicators of Shanghai metro network

Characteristic of Network	Calculated value for Shanghai metro
Node N	303
Link	350
Average node degree k^*	2.31
Characteristic path length L	14.87
Diameter of network D	41
Network cluster coefficient C	0.0082
Limit state of L ($\ln N / \ln k^*$)	6.82
Limit state of C (k^* / N)	0.0076

843

845
846

847　　Table 3 Ranking of node vulnerability

No.	Removed node	Vulnerability V	$V/E_f(\%)$	Node degree k
1	Caoyang Rd. Stn.	0.0073	7.37	4
2	Shanghai Railway Stn.	0.0066	6.69	4
3	Siping Rd. Stn	0.0065	6.57	4
4	Zhenping Rd. Stn.	0.0065	6.55	4
5	Longyang Rd. Stn.	0.0062	6.24	5
6	Yishan Rd. Stn.	0.0062	6.22	5
7	Century Ave Stn.	0.0062	6.22	8
8	Hongkou Football Stadium Stn.	0.0052	5.18	4
9	Luoshan Rd. Stn.	0.0050	5.08	4
10	Original Sports Center Stn.	0.0044	4.46	5

848

850
851

852   Table 4 R_e for different line recovery sequences

Recovery sequence[(*)]	R_e	Recovery sequence	R_e
2-6-9-4	0.974	6-4-2-9	0.968
2-6-4-9	0.973	4-2-9-6	0.967
6-2-9-4	0.973	4-6-2-9	0.967
6-2-4-9	0.972	9-2-4-6	0.966
2-9-6-4	0.971	6-9-4-2	0.965
2-4-6-9	0.971	4-9-2-6	0.964
2-4-9-6	0.970	6-4-9-2	0.964
6-9-2-4	0.969	9-4-2-6	0.964
2-9-4-6	0.969	9-6-4-2	0.963
4-2-6-9	0.969	4-6-9-2	0.963
9-2-6-4	0.969	4-9-6-2	0.962
9-6-2-4	0.968	9-4-6-2	0.962

853   Note: * Sequence 2-6-9-4 stands for the recovery sequence for metro line 2 as the first, line 6 as
854   the second, line 9 as the third and line 4 as the last.
855

857
858

859 Table 5 Best recovery sequence of metro lines for all exchange stations in Shanghai by

860 minimizing the resilience triangle.

Metro Station	Best metro line recovery sequence
Xujiahui Stn.	11-1-9
Shanxi Rd.(S) Stn.	12-10-1
People's Square Stn.	2-8-1
Hanzhong Rd. Stn.	1-12-13
Nanjing Rd.(W) Stn.	12-2-13
Longyang Rd. Stn.	2-16-7
Yishan Rd. Stn.	9-3-4
Oriental Sports Center Stn.	8-11-6
Caobao Rd. Stn.	12-1
Shanghai Sport Center Stn.	1-4
Changshu Rd. Stn.	7-1
Shanghai Railway Stn.	1-3
Zhongshan Park Stn.	2-3
Jiangsu Rd. Stn.	11-2
Jing'an Temple Stn.	2-7
Nanjing Rd.(E) Stn.	2-10
Longcao Rd. Stn.	12-3
Hongqiao Rd. Stn.	10-3
Jinshajiang Rd. Stn.	13-3
Caoyang Rd. Stn.	11-3
Zhenping Rd. Stn.	7-3
Hongkou Football Stadium Stn.	3-8
Hailun Rd. Stn.	4-10
Dalian Rd. Stn.	12-4
Lancun Rd. Stn.	4-6
Xizang Rd.(S) Stn.	8-4
Damuqiao Rd. Stn.	12-4
Dong'an Rd. Stn.	4-7
Jufeng Rd. Stn.	6-12
Gaoke Rd.(W) Stn.	7-6
Yaohua Rd. Stn.	7-8
Longhua Rd.(M) Stn.	7-12
Zhaojiabang Rd. Stn.	9-7
Changshou Rd. Stn.	7-13
Siping Rd. Stn.	10-8
Qufu Rd. Stn.	8-12
Laoximen Stn.	8-10
Lujiabang Rd. Stn.	9-8

Jiashan Rd. Stn.	12-9
Madang Rd. Stn.	13-9
Jiaotong University Stn.	11-10
Xintiandi Stn.	10-13
Tiantong Rd. Stn.	12-10
Longde Rd. Stn.	11-13
Longhua Stn.	11-12
Luoshan Rd. Stn.	16-11
Shanghai South Railway Stn.	1-3
Hongqiao Airport Terminal 2 Stn.	2-10
Baoshan Rd. Stn.	3-4

861

863

864 Table 6 Resilience index R_e for different recovery sequence of metro stations with different node

865 degrees.

Recovery sequence [(*)]	Re	Recovery sequence	Re
16-43-133-13	0.927	43-13-16-133	0.906
43-16-133-13	0.926	133-43-13-16	0.904
16-133-43-13	0.923	16-13-133-43	0.903
43-133-16-13	0.921	43-13-133-16	0.901
16-43-13-133	0.920	13-16-43-133	0.895
43-16-13-133	0.919	13-43-16-133	0.894
133-16-43-13	0.919	133-13-16-43	0.894
133-43-16-13	0.917	133-13-43-16	0.893
16-133-13-43	0.911	13-16-133-43	0.890
43-133-13-16	0.908	13-43-133-16	0.889
16-13-43-133	0.907	13-133-16-43	0.886
133-16-13-43	0.907	13-133-43-16	0.885

866 Note: * Recovery sequence 16-43-133-13 means the recovery for node 16 (Shanghai Railway
867 station) as the first, node 43 (Century Ave station) as the second, node 133 (Oriental Sports
868 Center station) as the third and node 13 (People's Square station) as the last.
869

871

872

873   Table 7 Resilience index R_e for different recovery sequence of stations with the same node

874   degrees.

Recovery sequence	Re	Recovery sequence	Re
15-39-8-13	0.969	13-8-39-15	0.965
39-15-8-13	0.968	39-8-13-15	0.965
15-8-39-13	0.967	13-8-15-39	0.965
15-13-8-39	0.966	13-39-15-8	0.965
15-39-13-8	0.966	39-13-15-8	0.965
13-39-8-15	0.966	13-15-39-8	0.964
39-13-8-15	0.966	8-15-39-13	0.964
15-8-13-39	0.966	8-39-15-13	0.963
39-8-15-13	0.966	8-15-13-39	0.962
13-15-8-39	0.966	8-13-39-15	0.962
39-15-13-8	0.966	8-39-13-15	0.962
15-13-39-8	0.965	8-13-15-39	0.962

875

877　　Table 8 Repair options for rebuilding a metro station in Shanghai

Procedure	Options	Cost (million RMB)	Duration (day)
Site investigation	crew1+equipment1	6	50
	crew2+equipment2	8	40
Pile foundation	crew1+equipment1	6	30
Retaining wall	crew1+equipment1	29	80
	crew2+equipment2	33	70
Excavation /support /dewatering	crew1+equipment1	15	180
	crew2+equipment2	20	165
Underground structure	crew1+equipment1	30	120
	crew2+equipment2	35	110

878

880 Table 9 Integrated repair duration and cost for rebuilding a metro station in Shanghai

Duration (day)	C_{repair}			$C_{disruption}$	C_{total}
	Direct Cost	Indirect cost	sum		
415	102.0	41.5	143.5	33.2	176.7
420	98.5	42.0	140.5	33.6	174.1
425	95.1	42.5	137.6	34.0	171.6
430	92.5	43.0	135.5	34.4	169.9
435	90.9	43.5	134.4	34.8	169.2
440	89.5	44.0	133.5	35.2	168.7
445	88.0	44.5	132.5	35.6	168.1
450	87.0	45.0	132.0	36.0	168.0
455	86.4	45.5	131.9	36.4	168.3
460	86.0	46.0	132.0	36.8	168.8

881 Note: *cost unit is million RMB.*

882

884
885

(a)

888
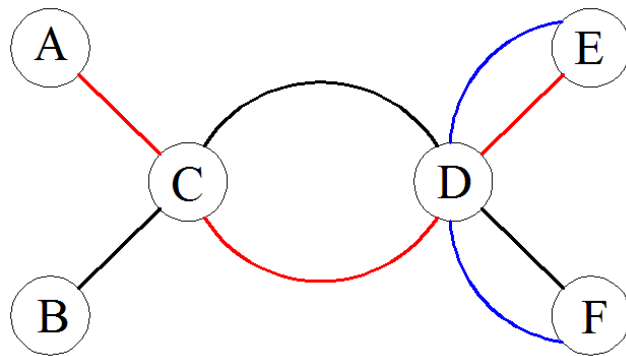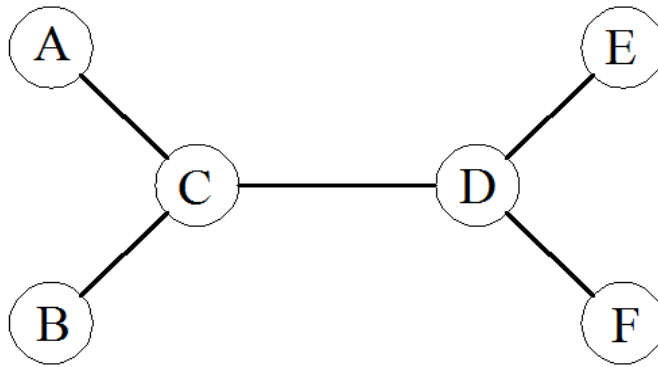
889   (b)

Figure 1. L-space type of topological graph for typical metro network: a) example of metro

network; b) topological graph corresponding to the metro network

893
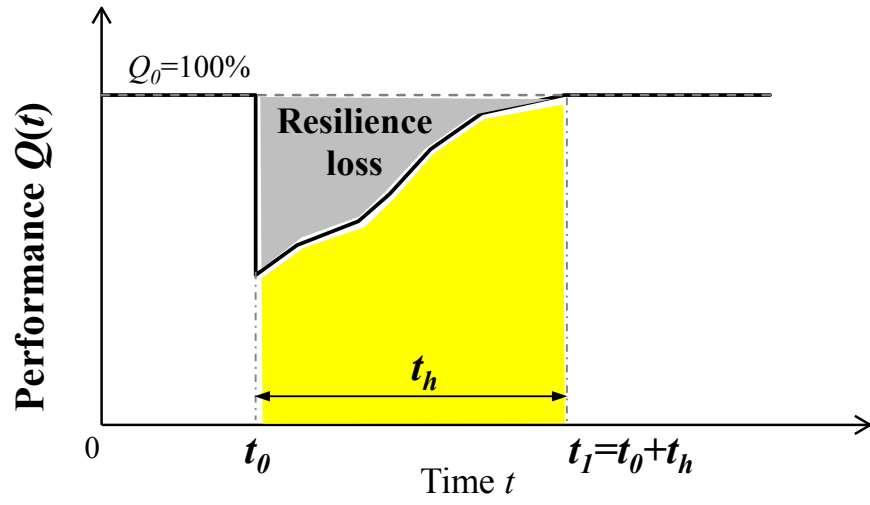
894

895   Figure. 2 Graphical measure of resilience including resilience loss triangle

(a)

(b)

899

900

(c)

(d)

901

902
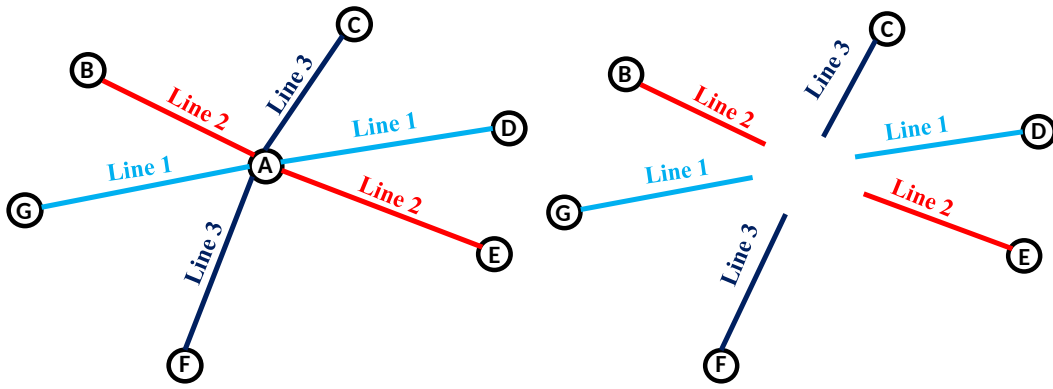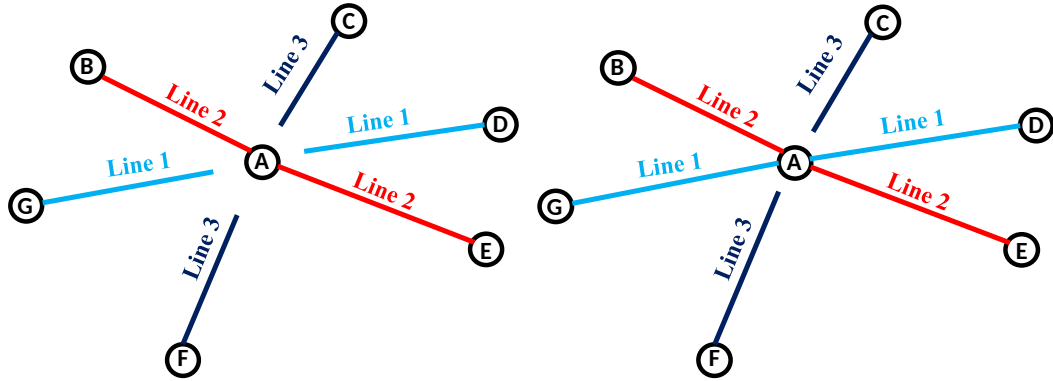
Figure. 3 Recovery strategy for a multi-line exchange station (three-line exchange as an example): a) original state; b) disconnected state; c) first stage of recovery; d) second stage of recovery;

903

904

905

907
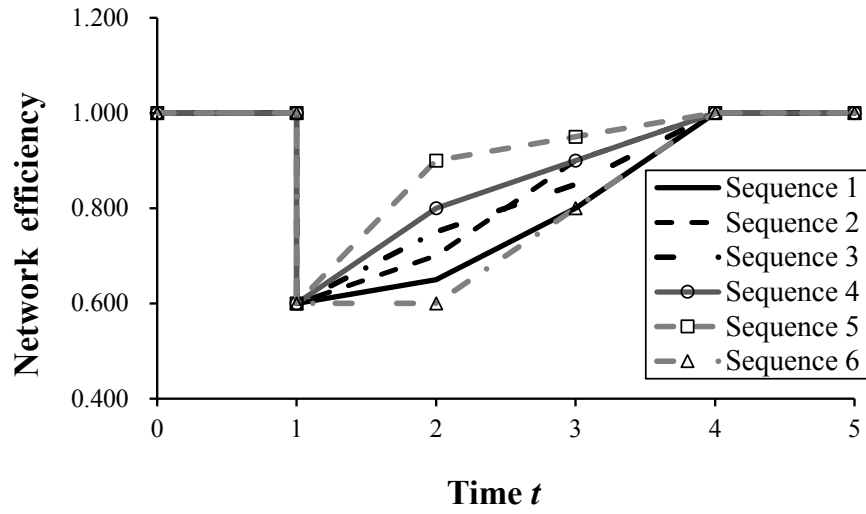
908

909   Figure. 4 Performance recovery curves corresponding to specific recovery sequence for node A

910   in Figure 3.

912

913

914   (a)

915
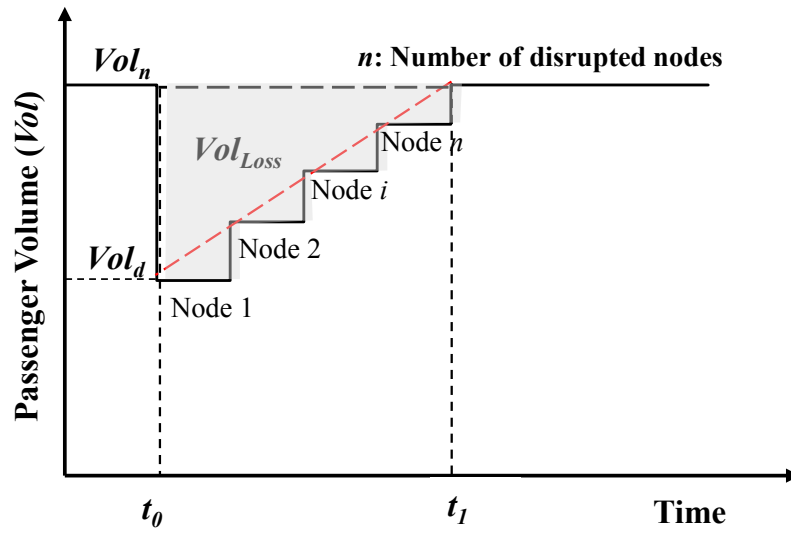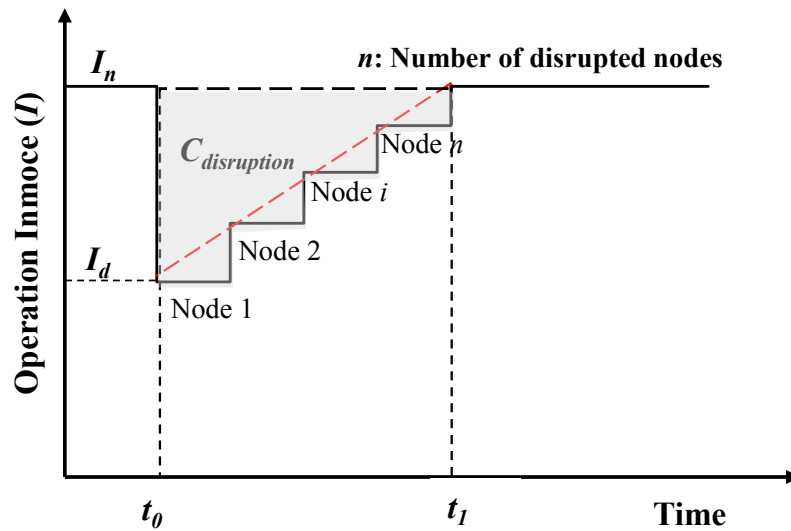
916   (b)

Figure 5 The time-dependent recovery curve of passenger volume and operational income: a)

passenger volume; b) operational income;

920
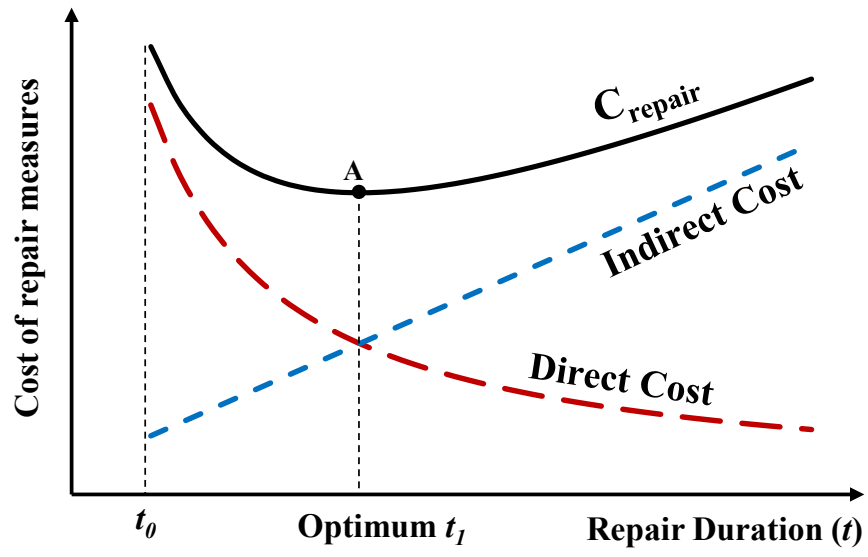
921

922   Figure 6 Cost of implementation of repair works including the direct cost and indirect cost.

924
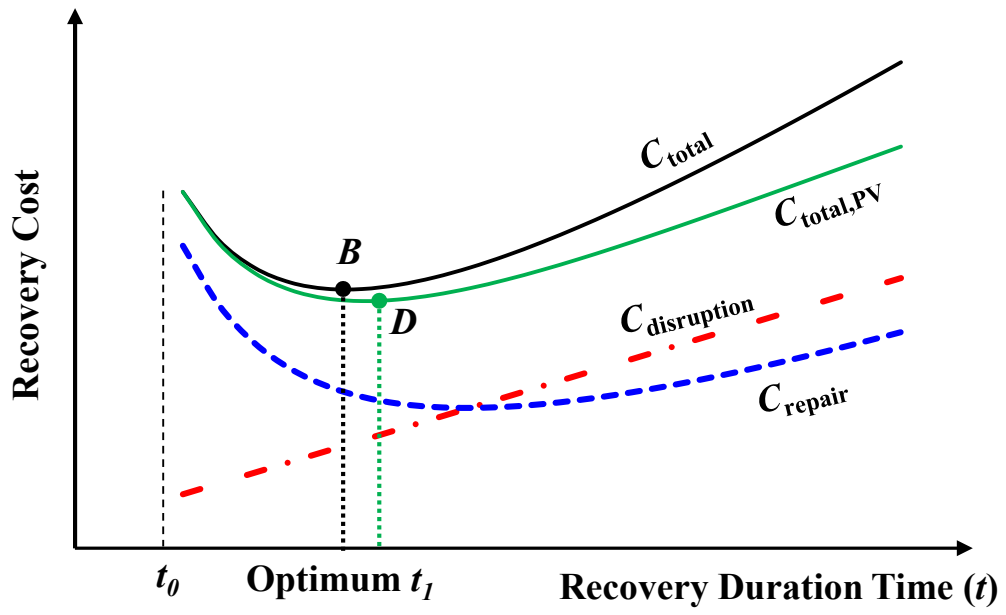
925

926   Figure 7 Time-cost curve for the recovery of a disrupted metro network

928
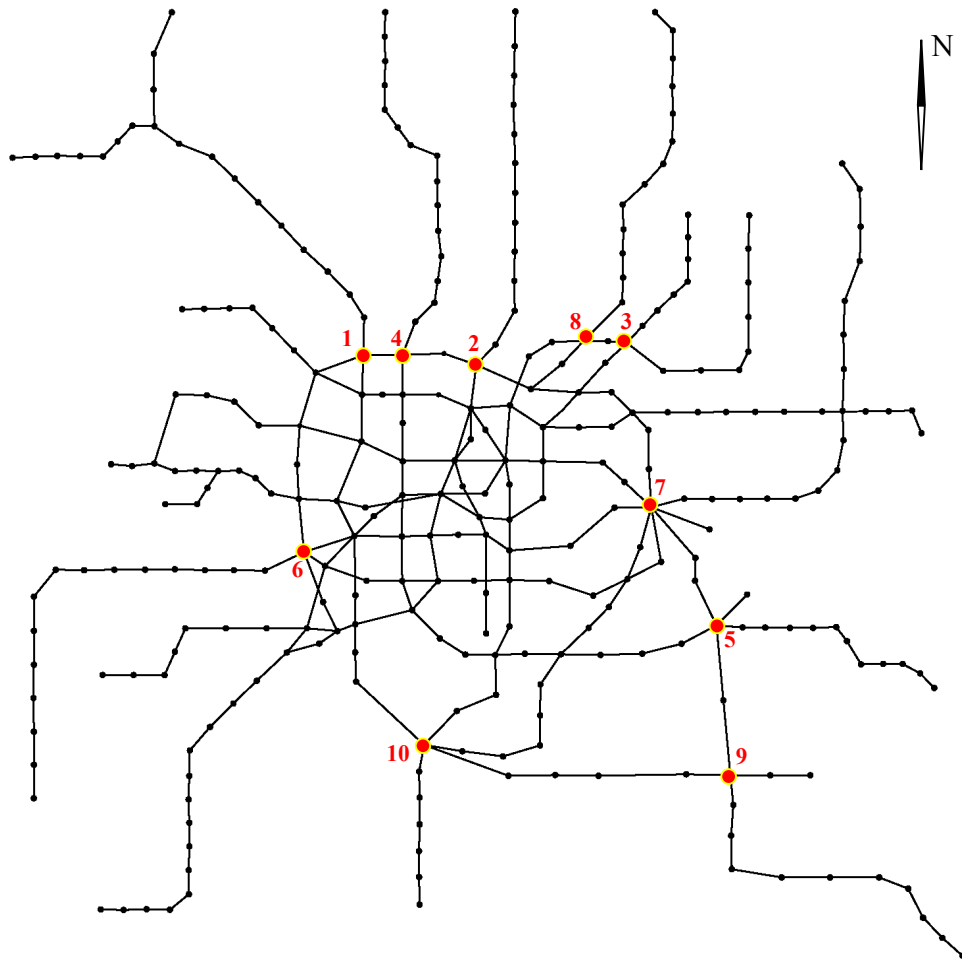
929

930　　　　　Figure 8 Typical topological network for the Shanghai metro system

932

933

934   (a)

$$p(k) = 3.858k^{-3.352}$$
$$(R^2 = 0.718)$$
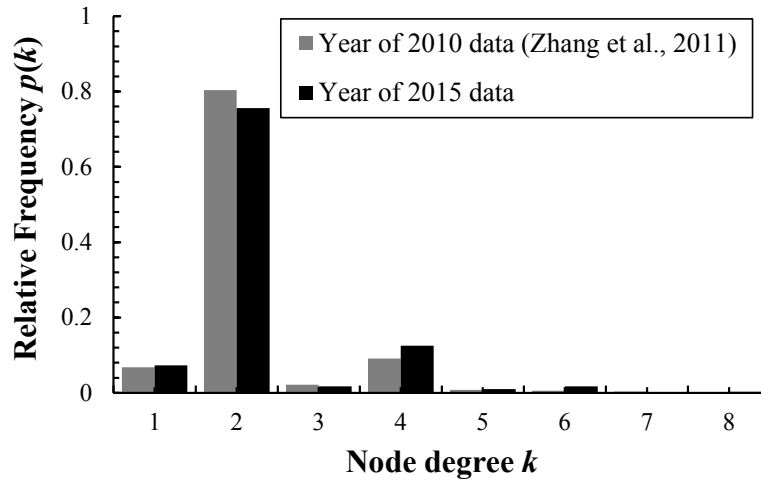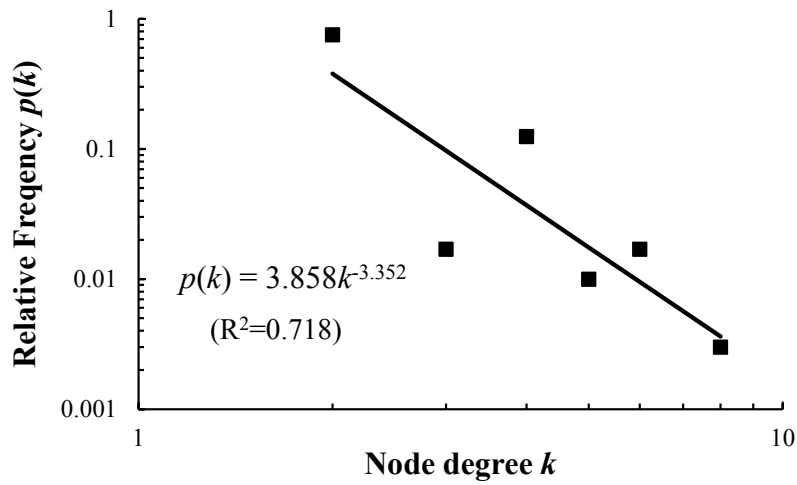
935

936   (b)

937   Figure 9 Distribution of node degrees for 303 metro stations in the Shanghai metro system: a)

938   histogram of k; b) linear fitting of the relative frequency of $p(k)$ with k for data from year of 2015

940
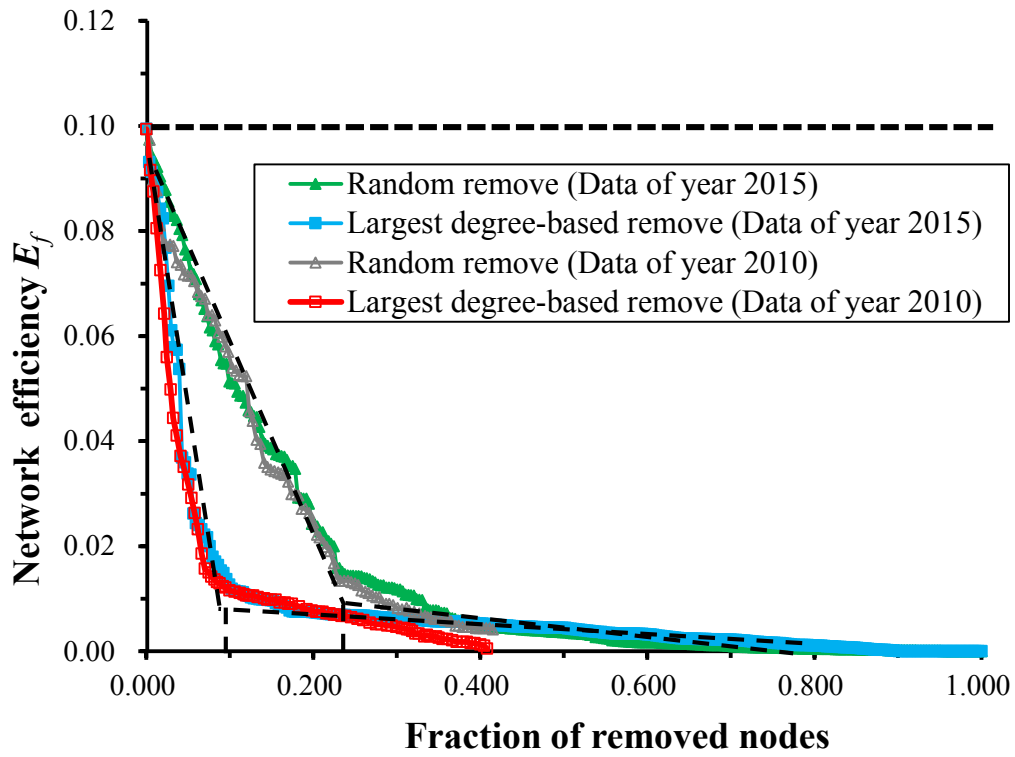
941

Figure 10 Robustness of the Shanghai metro network under different node removal type (Data

for year of 2010 is extracted from Zhang et al., (2011))

945

946
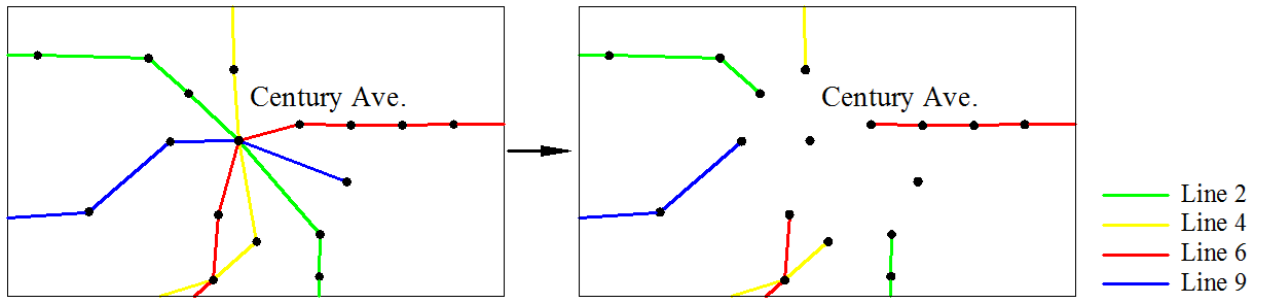
947
Figure 11 The effect of failure of Century Ave station on the surrounding network
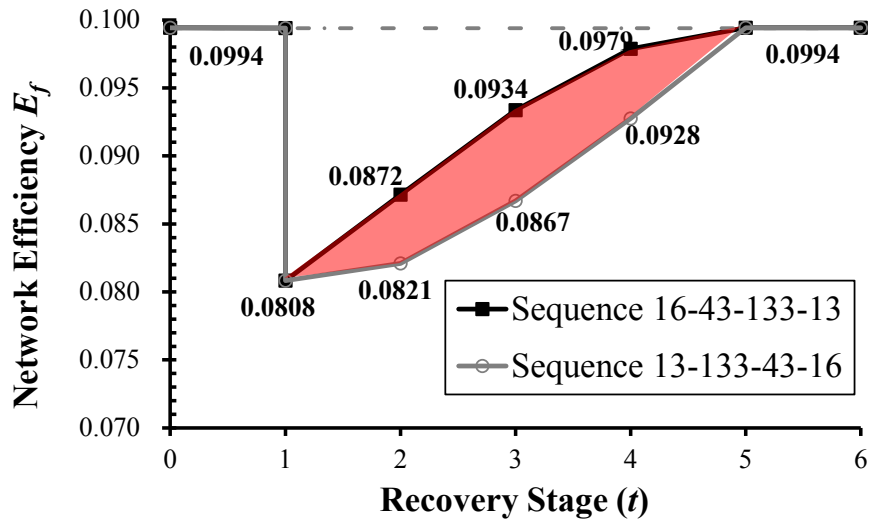
949
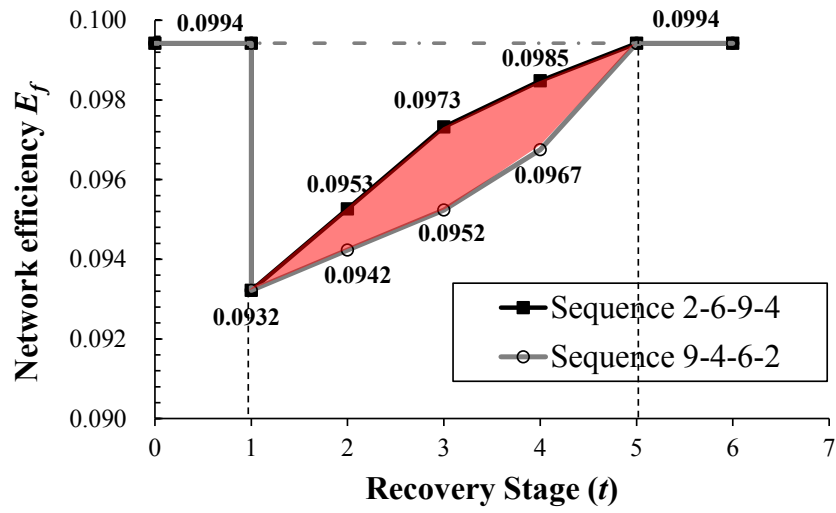
950

951   Figure 12 Comparison of change of network efficiency under two different recovery sequences

952   for recovering a multi-line exchange station.
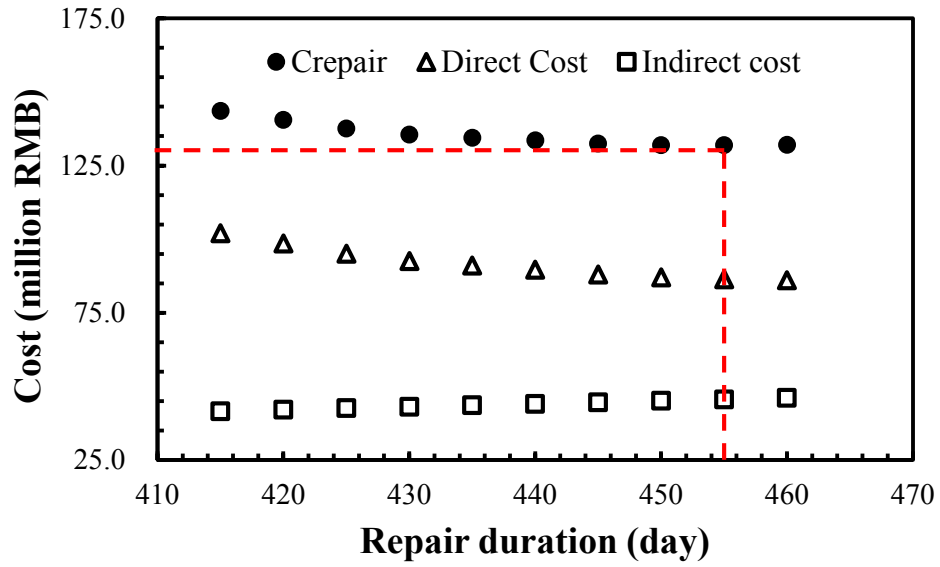
954

955

Figure 13 Comparison of change of network efficiency under two different recovery sequences

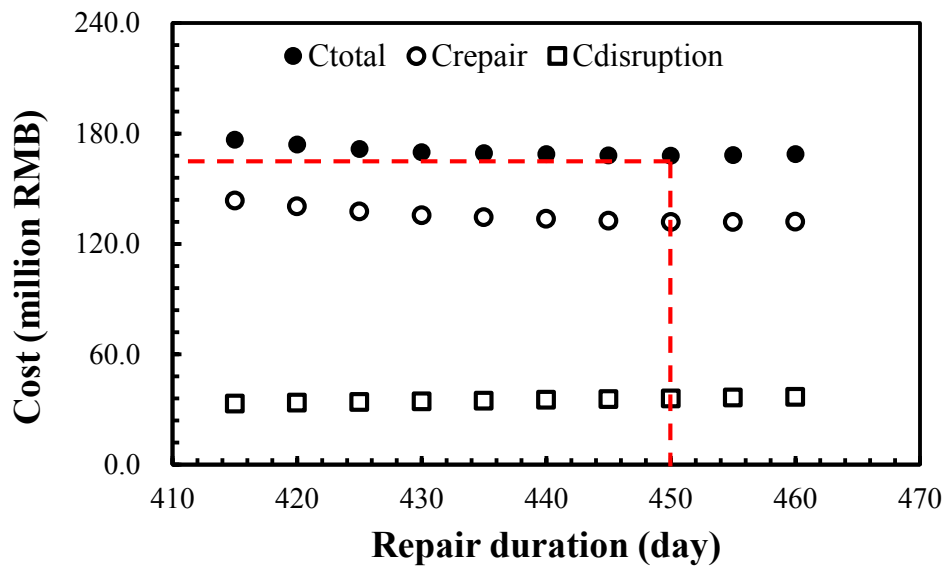for recovering a multi-line exchange station.

956

957
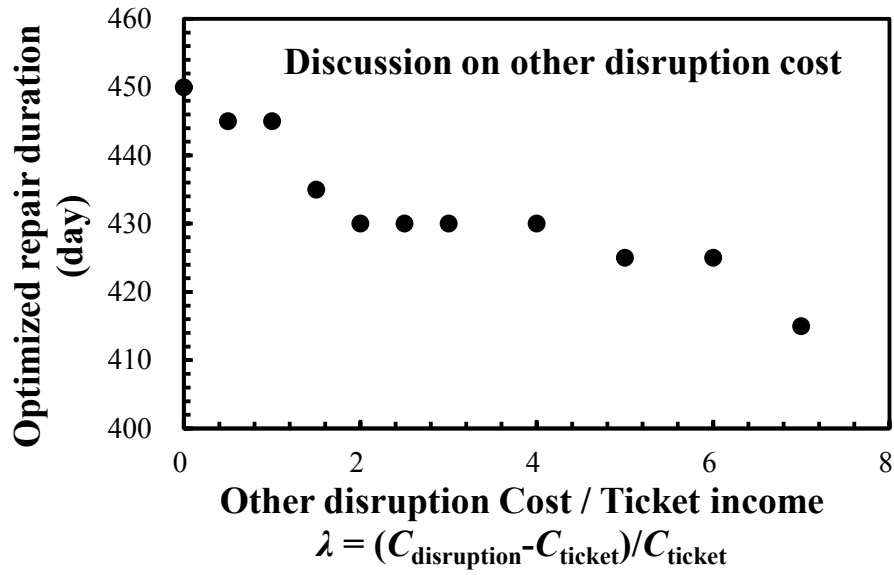
959

960

(a)

961

962

(b)

Discussion on other disruption cost

Optimized repair duration (day) vs. Other disruption Cost / Ticket income

$\lambda = (C_{\text{disruption}} - C_{\text{ticket}})/C_{\text{ticket}}$

(c)

Figure 14 Time-cost trade-off analysis for rebuilding a metro station: a) time-cost for repair cost; b) time-cost for total cost including disruption cost and repair cost; and c) effect of other disruption cost on the optimized repair duration days